CRASHWORTHINESS OF HIGH-SPEED RAIL SYSTEMS

A thesis

Submitted by

Laura Sullivan

In partial fulfillment of the requirements
For the degree of

Master of Science

In

Mechanical Engineering

TUFTS UNIVERSITY

November 2011

Adviser: Professor Douglas Matson

Abstract

Rail crashworthiness research focuses on the ability of passenger rail equipment to protect its occupants in the event of a collision. The goal of this research is to explore current high-speed trainsets and determine the level of structural crashworthiness they can provide to the occupant. One of the most effective ways of providing structural crashworthiness is through crash energy management. A crash energy management system (CEM) utilizes energy absorbing crushable elements and a strong vehicle structure to disperse collision energy in a controlled manner and provide protection to passengers. A survey of high-speed rail systems currently in operation was performed to determine appropriate equipment characteristics. An appropriate collision scenario was selected by reviewing accidents involving high speed equipment. Occupant safety was assessed by examining the performance of the equipment in the chosen collision scenario by using a one-dimensional lumped-parameter collision dynamics model to simulate a series of collisions. The features of interest are the energy absorbing capacity of the crush zone and the strength of the occupied volume and the influence that each of these features has on structural crashworthiness. Key results examined include the maximum collision speed without loss of occupant space, the distribution of crush throughout the cars of the train, and the severity of the deceleration experienced by the passengers.

Table of Contents

List of Appendices

List of Tables

List of Figures

1. Introduction

Multiple factors contribute to the overall safety of a rail system. Infrastructure, maintenance programs, and control systems are all in place to provide safe operation. Despite the best accident prevention measures however, accidents may still occur. A system safety approach includes not only accident prevention measures, but accident mitigation features as well. Accident mitigation features are in place to provide the last line of defense for passengers in the event of an accident. This thesis focuses on structural crashworthiness as the primary means of accident mitigation.

High-speed systems present new challenges to equipment design. In order to reach increasingly higher speeds, focus has been put on performance and lightweight construction. Increasing the speed cannot be the only focus however. Operating at these high speeds could increase the severity of collision conditions. Attention must be paid to the structural crashworthiness of the vehicles to provide safety for a changing environment.

The main goals of structural crashworthiness are to preserve occupant volume and limit the decelerations of the occupants to survivable levels. One of the most effective ways of achieving these goals is through crash energy management. A crash energy management system (CEM)

disperses collision energy in a controlled manner and provides protection to passengers. A CEM system is a combination of crushable elements that absorb collision energy on the ends of each car in the trainset, while a strong structure surrounds the occupied volume of the car. Energy absorption and occupant volume strength work together to mitigate the effects of a collision on the passengers.

The goal of this thesis is to explore high speed systems and describe the level of structural crashworthiness they can provide for the occupant. In order to achieve this, a brief history of the development of crashworthy structures and CEM systems is provided. The development of crashworthiness requirements and the resulting designs are discussed. A survey of high-speed systems currently in operation and proposed for operation is performed.

A model is then constructed to represent these high speed systems. Model variables describe the CEM system. The features of interest are the energy absorbing capacity of the crush zone and the strength of the occupied volume. The range of energy absorption capacities is obtained from reviewing available equipment information. The occupant volume integrity will be represented by a range in values that account for variation in strength requirements and construction.

The characteristics of the CEM system are defined in the model by a force-displacement characteristics at each vehicle end. Each variation in energy absorption capacity and occupant volume strength will be represented by alterations made to the force-displacement characteristic. In order to determine the level of crashworthiness these systems can provide, a collision dynamics analysis will be performed.

Model results include the distance that the end of each car crushes. Each piece of equipment will have a degree of allowable crush, but once this is exceeded occupant volume intrusion occurs. Comparing the distance each end crushes to the allowable crush demonstrates the ability of the equipment to preserve sufficient space for the occupants to ride out the collision. Results also include the decelerations of each car and the relative accelerations that the occupants experience; this will demonstrate if the equipment has limited the deceleration of the occupant volume to survivable levels.

An appropriate collision scenario is selected by reviewing accidents involving high speed equipment. Occupant safety is assessed by determining the safe speed of the equipment in the collision scenario. The safe speed is the speed at which no occupant volume intrusion occurs. A range of velocities will be investigated to determine the safe speed for each trainset. The resulting secondary impact velocity, the velocity with

which an occupant in free flight during the collision would strike the interior of the vehicle, is calculated to demonstrate the ability of the equipment to preserve occupant volume and limit the decelerations of the passengers.

2. Background

Railroad safety is a combination of accident prevention and accident mitigation. One of the most prominent accident mitigation elements is structural crashworthiness. The main goals of structural crashworthiness are to preserve occupant volume and limit the decelerations of the occupants to survivable levels. Occupant volume is preserved by creating a strong structure to protect the passengers, and the decelerations are limited by controlling the behavior of the trainset as it strikes an obstacle. Although this cannot be perfectly achieved for every collision scenario, design improvements can be made to increase the crashworthiness of the structure.

High speed operations are of concern to railroad safety due to the potential for more severe collisions. When moving objects collide and come to rest, the kinetic energy of the moving system is transformed. In the case of a trainset colliding with an obstacle, this transformation of kinetic energy can result in derailments, overriding, crushing, and buckling. The kinetic energy is a product of the mass and the velocity squared. Trainset masses do not vary much and will have less influence on the kinetic energy than speed. Variations in velocity are far more substantial and will have much more influence on the kinetic energy of the collision.

The traditional approach to structural crashworthiness is to construct cars that are strong enough to withstand collision forces. While this approach addresses the root cause of crushing, nothing is done to control the collision forces or the deceleration of the trainset. The collision forces may increase to the point of overwhelming the structure. Crushing of the structure and severe decelerations may lead to injuries and fatalities.

More recent approaches have focused on controlling the collision forces and the deceleration of the trainset in the collision. The strong structure surrounding the passenger is maintained, but the forces acting upon it are controlled through the plastic deformation of designated crush zones. As the crush zones collapse they absorb collision energy. These crush zones are designed to crush in a controlled manner to limit the collision forces on the structure and determine the load path of forces.

This approach to structural crashworthiness utilizes a CEM system. The goal of a CEM system is to absorb collision energy and control the collision forces so that crush occurs only in the crush zones and the occupied area remains intact. The kinetic energy of the collision can be dissipated by using a series of crush zones on the end of each car in the trainset. Multiple approaches have been taken to design CEM systems.

Although the focus and design methods vary, improvement to the crashworthiness of the structure are made in each case.

2.1. How is Structural Crashworthiness Achieved

The strong occupant volume is provided by the underframe and longitudinal members of the carbody. Many standards include a buff strength requirement that specifies a load applied along the line of draft. This requirement ensures that the structure does not permanently deform when forces are applied through the coupler in either service loading conditions or during collisions. The buff strength requirement and compressive loading requirements for the remaining longitudinal members require a structure that can resist crushing and protect occupants.

The crush zone is designed with crushable structures that collapse in a controlled manner. In this way, the collision loads can be limited as the structures collapse and transfer forces along a designated load path. These crushable structures will generally include operational features such as the draft gear and coupling equipment, as well as features dedicated to absorbing collision energy and controlling the collision forces such as energy absorbers.

Appendix 1 describes the characteristics of a CEM system in more detail and how forces are controlled during the collision. It includes a brief description of how these systems can be represented numerically. In addition, it describes the idealized function of the CEM system, and explains how load is managed before reaching the occupied volume.

In a collision, the leading car strikes the obstacle and begins to decelerate; as it does this the car trailing it will strike it from behind. Each successive car strikes the car preceding it. The overall collision behavior of the trainset is defined by this series of collisions that occurs down the length of the trainset. Multiple factors will contribute to the characteristics of this series of collisions. The gap, and coupling between the cars will influence the decelerations of each car in the trainset [1]. The strength of each car will influence the collision forces that the car trailing it experiences [2].

Variations in equipment configuration and philosophies have resulted in multiple approaches to CEM system design [3]. Design methods have included creating a crush zone capable of controlling the collision sequence such that each car experiences its own collision. In this way, the energy associated with the collision is divided to each vehicle in the trainset. Other methods have focused on creating a crush zone capable of controlling the collision such that the decelerations are all

limited to survivable levels. Crush zones are designed to ensure that the force levels allow for gradual decelerations of the occupied area. In each case the occupied area is protected by a strong structure that resists deformation. Consideration of the size and location of crush zones is important, in particular for cases where existing equipment is modified.

Each of these approaches has focused on a specific set of requirements, different types of equipment and a different collision scenario. Every operating environment will have a unique set of concerns; the presence of additional rail traffic, grade crossings, and historical accident data all play a role in characterizing these. Design improvements are made to address the most substantial of these concerns. Although each approach has focused on specific operating environments, the results are a step in the right direction towards improving the crashworthiness of equipment for a broader application. The resulting systems will not protect every passenger in every collision, but are capable of increasing the level of safety in a variety of collision scenarios.

2.1.1. Previous Research

The design philosophy based on the utilization of crush zones was proposed by researchers in the United Kingdom after a review of accidents and their consequences [4]. Initial studies focused on the

practical application of adding crush zones to existing equipment and developing computational methods for analysis [5]. The effectiveness of a single vehicle that could absorb collision energy in a controlled manner while maintaining survival space was demonstrated. It was concluded that designs including energy absorption could offer more protection than vehicles designed for strength only. Methods for computational analysis were developed and demonstrated to show close agreement with the full-scale tests.

This work was expanded upon to demonstrate that a trainset of coupled vehicles could safely absorb collision energy and distribute crush along the length of the trainset [6]. The ideal collision dynamic was one in which each car in the trainset collides and stops before the car trailing it begins to decelerate. The energy absorption at the colliding interface would be complete before energy absorption at trailing interfaces began. In this ideal case the colliding end would absorb twice as much collision energy as subsequent interfaces. Crush zones were redesigned to reflect the collision energy that would need to be dissipated at each end to create the ideal collision.

This idealized behavior allows for crush to be distributed through the trainset, but could not practically be achieved with resiliently coupled equipment. In practice, the colliding end would have to absorb most of the

collision energy while trailing interfaces were relatively unaffected. The inclusion of a deformable coupler however could more closely approximate the ideal collision behavior and more evenly distribute crush to each car end. A full-scale train-to-train test was then performed and it was demonstrated that the damage to the trainset could be controlled and focused on crush zones.

Research undertaken in the United States approached CEM development by determining the force-displacement characteristic necessary to limit the secondary impact velocities and preserve occupant volume. Survivable decelerations were determined for a specific collision scenario and a force-displacement characteristic was designed. Modifications were then made to the idealized force crush characteristics to account for physical constraints on the force levels and crush distances [7].

The resulting force crush characteristics were used to demonstrate that a CEM system could provide increased crashworthiness in a train to train collision when compared to conventional equipment. This approach optimized a CEM system for a prescribed collision scenario involving locomotive-led equipment. Some modifications were made so that additional collision scenarios could be evaluated. It was then demonstrated that a cab-led CEM system showed increased

crashworthiness performance when compared to conventional equipment in multiple collision scenarios [8].

Once the capability of a CEM system to improve crashworthiness was established for these limited cases, the influence of additional operational factors was taken into account [9,10]. This would establish robustness of the design in more varied situations, and demonstrate that it could be included in practical operations. This research compared consist type, car weight, and trainset length for both conventional and CEM equipment. The metric of safe speed, the maximum speed at which occupant volume is maintained, was used to compare the performance of each trainset in a collision with a locomotive-led freight consist. Consist-type comparisons showed that CEM trainsets operating in cab-led push-pull configurations had a slightly lower safe speed than trainsets configured as multiple units. Increases in car weight also showed a small decrease in safe speed, while the train length showed almost no effect on the safe speed achieved in the collision scenario.

Operational factors were further investigated to determine what strategies are effective at improving crashworthiness. This included the influence of cab-led vs. locomotive led operation for conventional and CEM systems [11]. The crashworthiness of each system was compared by determining the safe speed for collisions with identical trains. The level

of safety provided by conventional equipment was first established. For cab-led conventional equipment, the cab car experiences the most crush and occupant volume intrusion occurs at the colliding end. Locomotive-led conventional equipment had a higher safe speed. Damage to the trainset occurred at the first coach car coupled behind the locomotive. Additional crashworthiness strategies including full and incremental CEM were then compared to the baseline established by cab-led conventional equipment.

Minor adjustments to the system were represented by an incremental CEM system. In this case, a CEM cab-car led conventional coach cars that had been modified to include pushback couplers. This incremental CEM system achieved equivalent crashworthiness to a locomotive-led conventional trainset. For incremental CEM, crush is distributed to both the cab car and the first passenger car. The inclusion of a full CEM system increased the safe speed even further. As in the conventional case, the locomotive-led CEM trainset achieved a higher safe speed than cab-led CEM equipment.

It was established that a CEM system was effective at providing improved structural crashworthiness. Variations in operational factors had been accounted for and it remained to determine the influence of variations to the crush zone characteristics. Alterations were made to the

crush zone and the occupied volume strength. The crush zone consisted of a draft gear, pushback coupler, and energy absorber. The force levels of each component in relation to one another and the stroke length of the primary energy absorber were investigated [10]. The force level of the coupler, energy absorber and occupant volume were varied independently. The length and slope of the energy absorber were also varied. The safe speed was used to compare results for collisions with a locomotive-led freight consist.

It was observed that the safe speed remained nearly constant for small changes in occupant volume strength when the coupler and energy absorber force levels remained the same. The safe speed was more sensitive to changes made to the crush zone characteristics. Changes were made independently to the energy absorber force level and the pushback coupler force level. These changes made to the relative force levels of the crush zone features did result in changes in safe speed.

In addition to the level of force maintained by each component of the CEM system, the influence of energy absorber stroke length on safe speed was determined. When the stroke length of the energy absorber was increased, there was an increase in safe speed. The safe speed increased even further when the energy absorber was given a positive slope while maintaining the same average force level. This slope, by

decreasing the initial force of the energy absorber encouraged crush initiation and resulted in more crushing and utilization of the crush zone.

Further research varied crush zone and occupied volume characteristics with the intent of optimizing crush zone performance [12, 13]. The crush zone consisted of a draft gear, pushback coupler, and energy absorber. Adjustments were made each of these features and the occupied volume. Unlike previous studies, particular attention was paid to the energy absorption capacity of the crush zones. Alterations were made such that the area under the curve remained the same. The safe speed results of a collision with a locomotive-led freight train were then compared. Additionally, the timing between crush zone activation for each end in the trainset and the distribution of crush to each end in the trainset was described.

The components of the CEM influence the collision behavior of the trainset. The timing of the collision was affected by changes made to the draft gear and pushback coupler. The length of the draft gear influenced interactions between facing crush zones. Draft gears shorter than 3 inches caused near simultaneous activation of pushback coupler crush in facing crush zones. This resulted in a decrease in safe speed. The force level of the pushback coupler influenced the crush experienced at either end of an individual car. Decreasing the force level of the pushback

coupler caused quicker exhaustion of the pushback coupler and loading of the primary energy absorber. The pushback coupler on the front of the car will exhaust and loading of the primary energy absorber will begin before the pushback coupler on the rear of the car is exhausted. This resulted in a slight increase in safe speed.

In addition to the timing of the collision, the distribution of crush to each vehicle was influenced by the characteristics of the crush zone. It was demonstrated that the ratio of the average force level of the primary energy absorber to the force level of the pushback coupler effects the utilization of each crush zone. Increasing the average force level of the primary energy absorber and shortening the length of stroke resulted in an increase in crush zone utilization. When more of the crush zone is utilized, more collision energy can be dissipated safely. This increase in utilization resulted in an increase in safe speed.

Finally the robustness of the CEM system was analyzed [14]. Variations were made to each car end independently to determine the effect on the performance of the entire trainset. Variations of ± 20% were made to the average force level of the energy absorber and ± 50% to the force level of the pushback coupler. It was concluded that a reduction in force level encouraged crushing at that end and an increase in force level resisted crushing. This behavior was localized and had less of an effect

on surrounding interfaces in the trainset. The safe speed of the trainset was not greatly affected by the slight variations made at each end.

Up to this point research has focused on demonstrating that the inclusion of a CEM system can be effective at increasing the safe speed for multiple collision scenarios. The characteristics of the crush zone have been investigated to determine which features optimize energy absorption. This research seeks to broaden the scope and look at the major attributes of the CEM system. The effects of energy absorption capacity of the crush zone and strength of the occupied volume on structural crashworthiness will be described. By determining the influence of these CEM components, inferences can be made about the crashworthiness of existing high speed equipment.

2.1.2. Existing Technology

CEM technology has been developed and implemented in Europe and the United States, and multiple approaches have been taken. Each operating environment has a unique set of concerns and history that has dominated the development of safety improvements. Standards and requirements describe an acceptable level of safety performance that equipment must meet. In many cases, equipment is capable of exceeding these requirements, but a minimum level of performance is established.

Standards may include design requirements that specify the occupant volume strength and energy absorption capacity, or performance requirements that can be met by equipment with a range of energy absorption capacities and occupant volume strengths.

In the United Kingdom, British Rail (BR) developed a crashworthiness standard after a survey of accidents and their consequences. This crashworthiness standard included a design requirement of 7.4×10^5 ft lbs (1 MJ) of energy capacity at the end of each car [15]. These energy absorbers were added to equipment already meeting a requirement for a buff strength compressive load of 450 kips (2000 kN) [21]. This requirement did not take into account any variation in weight or collision speed, although it applied to a wide range of equipment. It was eventually adjusted to include an alternative collision scenario that could be applied to fixed consist trains [16]. Most recently, the performance standard has been updated to reference the European standard for crashworthiness which includes a range of prescribed collision scenarios [17]. These performance requirements can be fulfilled by a variety of CEM designs

In France, the Société Nationale des Chemins de fer Français; (SNCF) developed a requirement for modifying its high-speed equipment. A reference collision was developed based on a grade crossing collision that occurred in Voiron on September 23, 1988. The reference collision is a 68

mph (110 kph) collision with a 1.8 x 10^5 lb (80 ton) obstacle [18]. The resulting vehicle design for the TGV Duplex [Figure 1] focuses on the front end of the trainset, with large crush zones and increased occupant volume strength in front of occupied areas. The articulated interfaces absorb relatively little energy since the articulation prevents substantial inter-car collisions [3].

Figure 1: TGV Duplex Schematic

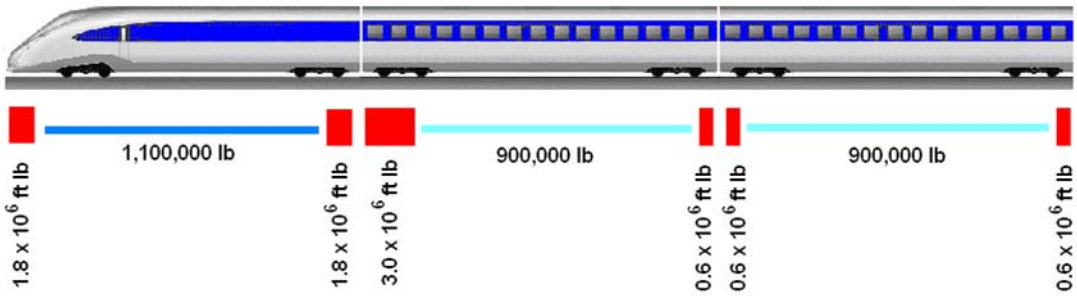

In the United States requirements were developed for high speed operation between speeds of 125 and 150 mph. This equipment must meet the design requirements and a collision scenario in the CFR [19]. The regulation specifies energy absorption capacities and buff strength requirements for each car in the trainset [Figure 2], as well as the inclusion of a locomotive at each end. The large frontal crush zone resembles that of the TGV and the conventionally coupled intermediate ends require moderately sized crush zones for inter-car collisions.

Figure 2: Acela Schematic

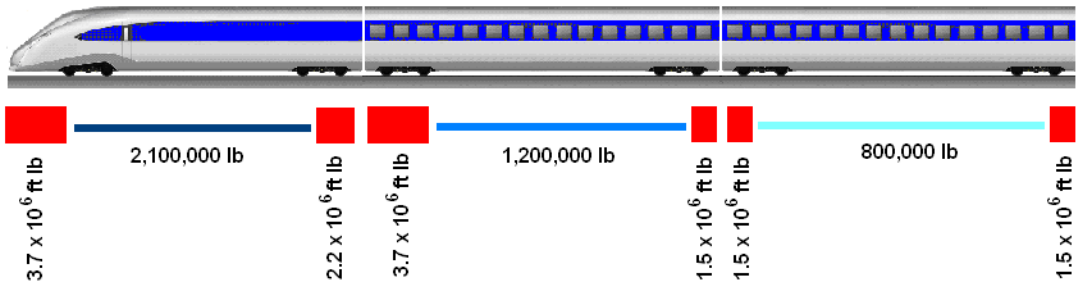

A wide range of high-speed equipment, equipment that operates at speeds in excess of 125 mph, is currently in operation. A survey of this equipment is contained in Appendix 2. This survey compiles information on CEM equipment, both high speed and conventional speeds and is intended to provide a snapshot of what CEM systems exist and where they operate. In addition to providing general information, details on trainset configuration, collision energy capacity and buff strength requirements will contribute to model characteristics used for analysis.

High speed equipment has been designed to meet various operational and crashworthiness requirements. A range of energy absorption capacities and occupant volume integrities exist for compliant equipment. In each case the combination of energy absorption capacity and occupant volume strength provide the necessary structural

crashworthiness to meet these requirements. Safety features have been included without undermining operational requirements.

2.2. Analysis Techniques

Analysis techniques have been developed to allow for design improvements to be analyzed without the expense of a full scale test. The crashworthiness of a CEM system can be determined using a collision dynamics analysis. Collision dynamics analyses model the motions of the trainset, the decelerations that each car in the trainset experiences, and the crush experienced by each car.

Collision dynamics analyses can be performed using a lumped parameter model, finite element model, or a combination of those two. A lumped parameter method simplifies the system into a series of masses and connectors. A finite element method can represent the complexities of the individual geometries by using more detailed structures. A combination of these two methods may model the features of interest using a more detailed model and use a simplified mass-connector model for the remainder of the analysis [20].

The simplest analysis is a one dimensional lumped-parameter model. This type of model is suitable if movement in other directions is limited. CEM

systems are designed to keep the trainset in line as it collides, so an analysis of only the longitudinal behavior is appropriate.

In a lumped parameter model the mass of each car is represented by a rigid body. The rigid bodies are connected by springs describing the collapse behavior of the carbody. The spring characteristics are defined by a force displacement curve. Appendix 3 describes how a force-displacement curve can be created for specific equipment. It includes examples for determining the force displacement characteristic using component information and full-scale test data. A simplified force-displacement characteristic is provided.

2.3. Analysis Goals

For this thesis a collision dynamics analysis is used to determine the level of crashworthiness that can be provided by high speed CEM equipment. The CEM system includes an energy absorbing crush zone and a strong occupied volume. These components of the CEM system affect the ability of the passengers to ride out the collision safely. The level of crashworthiness is determined by comparing the maximum speed at which the passengers can be protected from crushing, and if the forces on the passengers during the collision are limited.

The analysis variables are the energy absorption capacity and the occupant volume integrity. Two strategies are utilized for varying the energy absorption capacity. One strategy is used for varying the occupant volume integrity. Each variation is assessed by determining the safe speed, the secondary impact velocity (SIV) and the utilization. The SIV is the relative velocity of the occupant with respect to the interior of the occupied volume. The utilization is the percentage of CEM energy capacity that effectively absorbs energy during the collision.

The trainset used in this analysis is intended to be representative of existing equipment. The energy absorption capacity varies over a range of values that include equipment currently in operation. The occupied volume integrity is varied to represent the range in buff strength requirements. The analysis includes cases where the lead car has increased occupant volume integrity to represent trainsets that feature stronger leading cars. The safe speed and the secondary impact velocity will be determined for each variation.

3. Approach

The collision scenario should represent the loading condition that is most likely to occur in the collision of high-speed equipment. In order to determine an appropriate collision scenario, an accident survey was performed and is included in Appendix 4. This survey compiles details of accidents involving high speed equipment. The operating environment, the conditions of the accident and the equipment involved describe the type of accident. The outcome to the passengers and equipment describes the severity of the accident.

This thesis focuses on the in-line collision of equipment. After reviewing the collisions in Appendix 4, it was determined that a collision involving longitudinal loading is the most likely scenario. In collisions involving longitudinal loading passenger fatalities and injuries are mainly attributed to loss of survival space [21]. A one-dimensional lumped-mass collision dynamics model of a trainset into a rigid wall was analyzed [Figure 3]. This analysis represents the worst-case loading condition for the trainset; no energy is absorbed by the wall. The collision variables have been reduced to isolate the longitudinal collision behavior of the trainset.

Figure 3: Collision Schematic

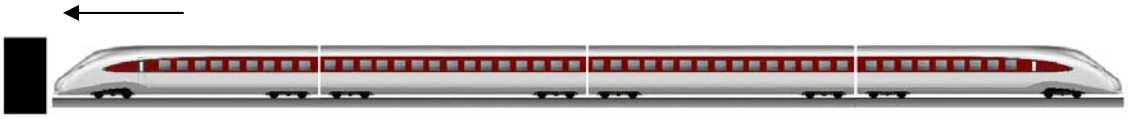

Results from the analysis determined the crashworthiness of the vehicle design and the performance of the CEM system. The crush data was compared to the amount of allowable crush to determine the safe speed. The safe speed is the maximum speed at which the occupant volume remains preserved. The velocity data was used to determine if the decelerations of the passengers were limited to survivable levels.

A series of assumptions were made to create a model that represents a high-speed trainset. A baseline CEM system was created using a simplified force-displacement characteristic. Incremental adjustments were made to energy capacities and crippling loads using multiple methods to account for ranges in equipment design. Each strategy for adjusting the force-displacement characteristic represents the alternatives available for changing the physical components of the crush zone. For each energy capacity, the crippling load was adjusted uniformly for each car in the trainset. For the baseline energy absorption capacity additional cases were modeled in which the leading car possesses a higher crippling load than the trailing cars.

Trainset lengths for equipment included in Appendix 2 varied from 4 to 16 cars. Trainset length for these analyses was limited to 4 cars. It has been demonstrated that the collision energy imparted to the colliding end and second interface were similar for train lengths of 4 to 8 cars [6]. Additional research demonstrated that the number of cars in a trainset does not influence the forces that the cars will be subjected to in a train to train analysis [22], and has a minimal effect on the safe speed of the trainset [9]. Due to the limited influence of the trainset length, and the largest proportion of collision energy being imparted to the colliding end, it was assumed that a four-car trainset could be used to represent the crashworthiness of longer trainsets.

The weight remained the same for each analysis. The influence of weight on safe speed is minimal [9]. Each car in the trainset was the same weight. From a review of existing equipment it was determined that car weight could vary from approximately 50,000 lbs to 150,000 lbs [Table 7]. Each car in the model weighed 95,000 lbs (43,000 kg).

Energy absorption capacity for the trainset was determined by reviewing the equipment included in Appendix 2. The energy capacity for the first four interfaces was calculated and values ranged from approximately 2,200,000 ft lbs to 15,000,000 ft lbs [Table 7]. For the baseline model of 4 cars, total trainset energy was 10,625,000 ft lbs. The

trainset energy capacity was distributed to the colliding and non-colliding ends of the trainset.

The energy absorption capacity on the colliding end was four times greater than the energy absorption capacity at each end. This distribution of energy absorption capacity was selected to accommodate the expected collision energy distribution. Figure 4 shows a schematic of the trainset with the ends and interfaces labeled. Interface A comprises the colliding end of the vehicle and the rigid wall. End #1 is the colliding end. Each trailing interface comprises two ends; these are the non-colliding ends. In an idealized collision, energy absorbed at the first interface will be two times greater than energy absorbed at trailing interfaces [1]. This ideal distribution of collision energy was demonstrated to be a good approximation for equipment with pushback couplers [6]. For this reason the each non-colliding end will posses 25% of the colliding-end energy absorption capacity for a total interface capacity of 50%.

Figure 4: Trainset Schematic with Locations labeled

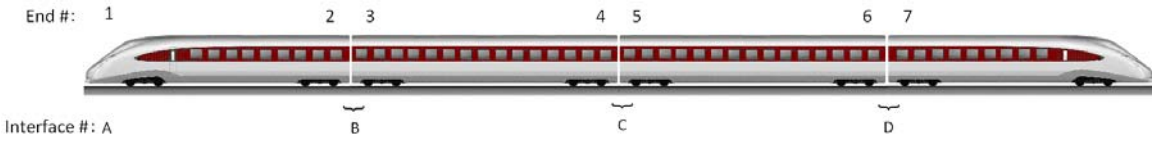

3.1. Force-Displacement Characteristics

Each car in the trainset has a nonlinear force-displacement characteristic associated with each end to describe the CEM system. These force-crush characteristic include the energy absorbing elements and occupant volume integrity. A wide range of equipment is intended to be represented so the crush zone includes only the basic features of the draft gear, pushback coupler, and primary energy absorber. Figure 5 shows a schematic of these elements of the crush zone on the vehicle end.

Figure 5: Crush Zone Schematic

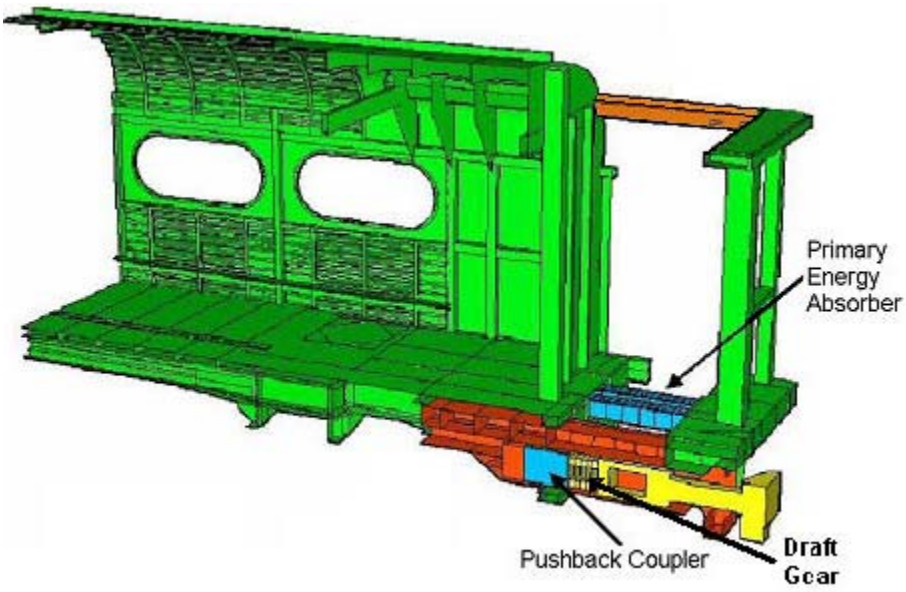

The force-displacement characteristic was simplified so adjustments could be made easily. The first portion of the simplified force-displacement curve shown in Figure 6, contains the draft gear, pushback coupler, and primary energy absorber and represents the crush zone. The area underneath this portion of the curve is calculated to determine the energy absorption capacity of each end. The peak force on the force displacement curve represents the crippling load of the occupied volume. The crippling load is the maximum force supported by the structure, once it has been exceeded the occupied area begins to crush. The characteristic for each element in the CEM system is discussed in detail.

Figure 6: Generic Force-Displacement Characteristic

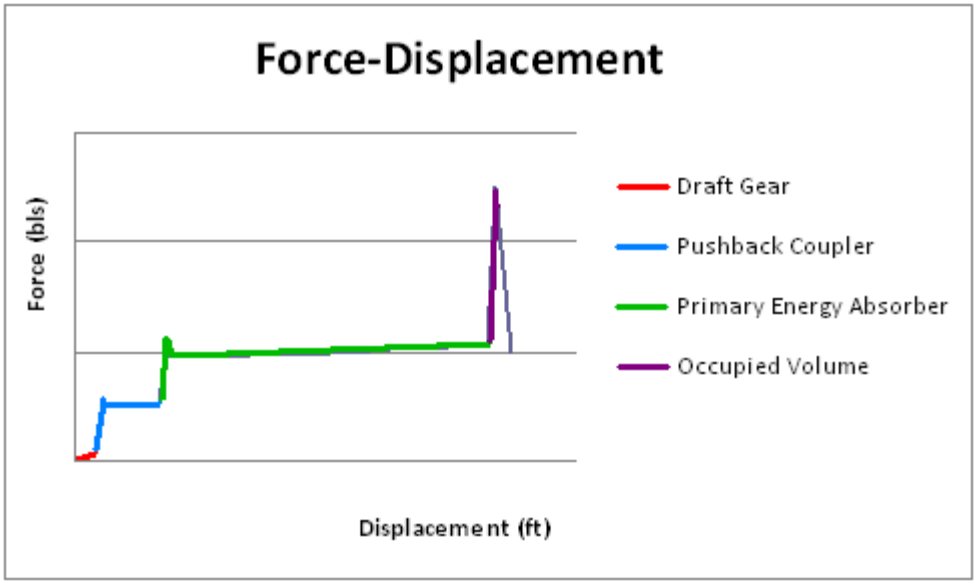

3.1.1. Baseline Force-Displacement Characteristics

The first element of the CEM system is the draft gear. The draft gear remains the same for each end for the entirety of the analysis. The draft gear is three inches in length and increases linearly to reach a maximum force value of 80,000 lbs (360,000 N) providing energy absorption of 10,000 ft-lbs (14 kJ) [Figure 7]. Previous research has demonstrated that the draft gear will play an important role in the timing of the collision behavior [13]. After the draft gear exhausts, force is transferred to the pushback coupler.

Figure 7: Draft Gear Force-Displacement

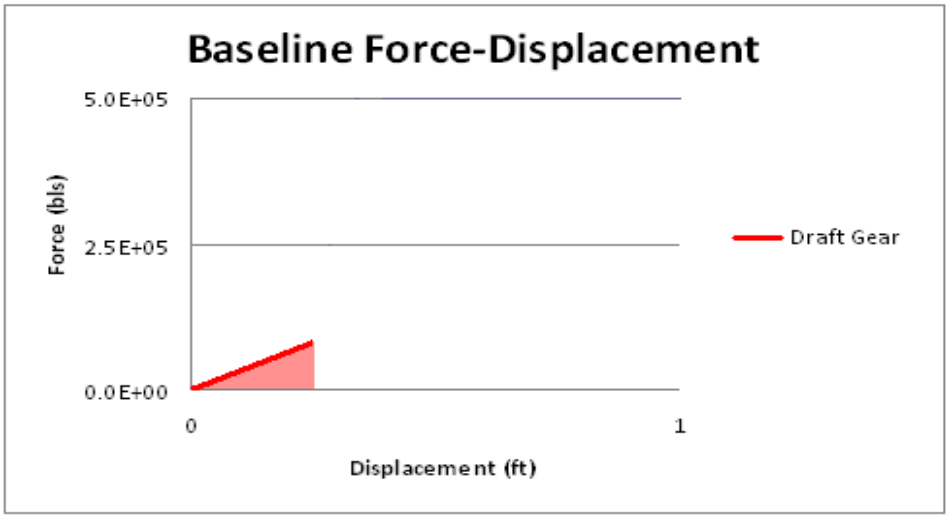

The pushback coupler for the colliding end [Figure 8] has a stroke length of 9 in. (23 cm), and the average force is 500,000 lbs (2.2 MN) after activation. This value remains constant for the remainder of the stroke

length. The activation force, circled in Figure 8, is 10% higher than the average force. The activation force represents the slight overshoot as the system transitions to a higher force level. This peak is slight enough that it does not prevent crushing of the stage. The colliding end pushback coupler provides energy absorption of 4.64 x 10^5 ft-lbs (629 kJ).

Figure 8: Collision-end Pushback Coupler Force-Displacement

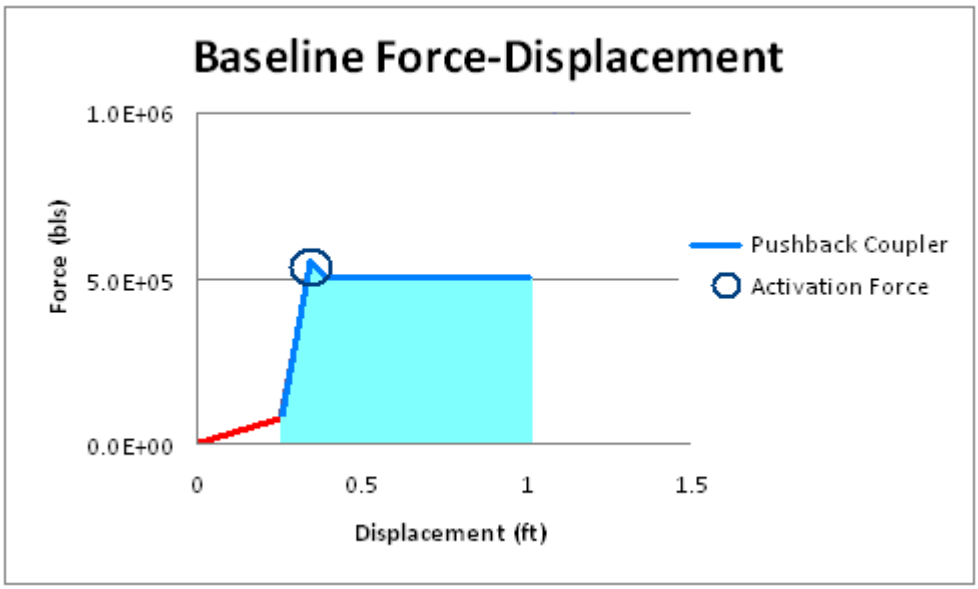

The pushback coupler on the non-colliding ends is modified from the colliding-end pushback coupler. The stroke length for non-colliding ends is decreased to 5 in. (13 cm). Pushback coupler force levels remain the same for colliding and non-colliding ends. The non-colliding end pushback coupler provides energy absorption of 2.99 x 10^5 ft-lbs (405 kJ). The non-colliding end pushback coupler is smaller than the colliding-end pushback coupler. Non-colliding ends experience face-to-face crushing

with other crush zones, the colliding end has to compensate for collision with a rigid object. After the pushback coupler exhausts, force is transferred to the primary energy absorber.

The primary energy absorber (PEA) for the colliding end has a stroke length of 4ft. (1.2 m) [Figure 9]. The average force of the PEA is 1,000,000 lbs (4.4 MN). This value is selected to be twice the average force of the pushback coupler and demonstrated efficient crushing in previous research [23]. The energy absorber should have a slight positive increase in slope to encourage crushing at initiation and allow for a gradual increase in force supported by the structure [10]. Values ranged from 950,000 lbs. (4.2 MN) after activation to 1,050,000 lbs. (4.7 MN) at exhaustion, providing a ± 5% range. The activation force, circled in Figure 9, is 10% higher than the average force. The colliding end PEA provides energy absorption of 3.776×10^6 ft-lbs (5 MJ).

Figure 9: Baseline Collision-end PEA Force-Displacement

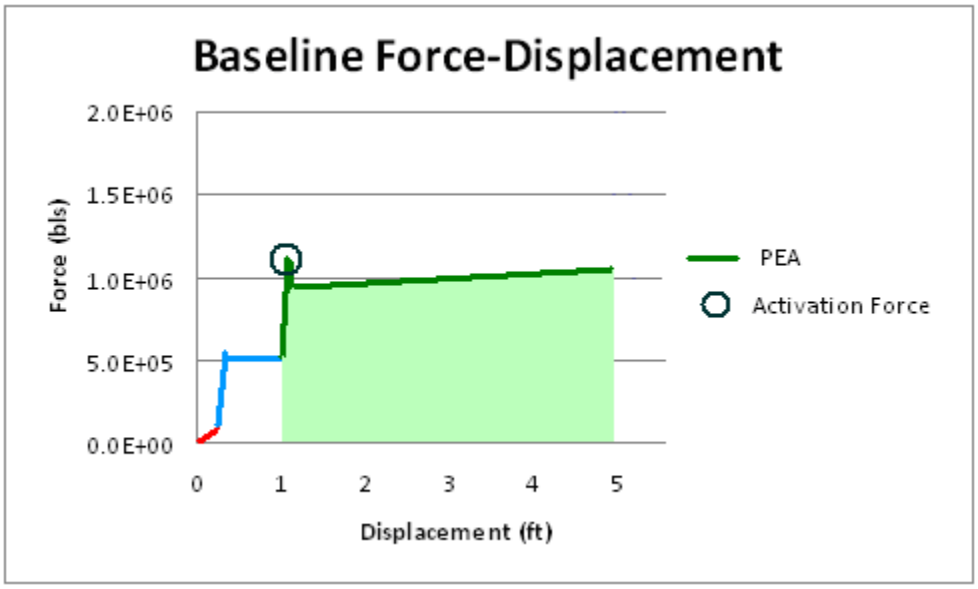

The primary energy absorber for the non-colliding end is also modified from the colliding end design. The stroke length is reduced to 1 ft. (0.3 m) for non-colliding ends. PEA force levels remain the same for colliding and non-colliding ends. This allows for the total energy capacity of the non-colliding end crush zone to be 25% of the colliding-end crush zone. This distribution of energy capacity is intended to accommodate for the distribution of collision energy during the collision. The energy capacity of the non-colliding end is 7.535 x 10^5 ft-lbs (1 MJ). Once the primary energy absorber is exhausted, the crush zone has been utilized. After the crush zone has completely deformed, forces are transferred to the final feature of the CEM system, the occupant volume.

The occupant volume strength is described by the crippling load point on the force-displacement curve. Figure 10 shows the force-displacement curve for the CEM system including the crush zone and occupied volume. The crippling load, circled in red in Figure 10, is located on the force-displacement curve 2.4 in. (6 cm) from the point of exhaustion of the crush zone. For the baseline case, the crippling load was 2.5 x 10^6 lbs. (11 MN). This value was the same for colliding and non-colliding ends. This value is representative of the crippling load for a conventional car meeting the 800,000 lb buff strength requirement. It was determined using full-scale test data [24]. The occupied volume provides an additional 1.775 x 10^5 ft-lbs (240 kJ) as it deforms before crippling. This additional contribution is negligible in comparison to the energy absorbed by the crush zone

Figure 10: Baseline Occupant Volume Force-Displacement

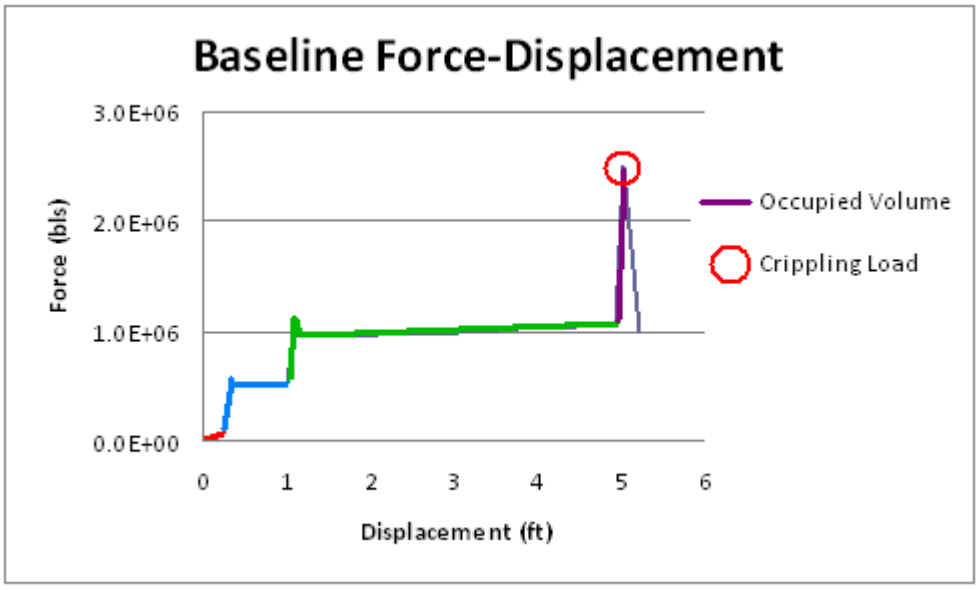

The baseline force-displacement characteristics for the colliding and non-colliding ends are shown in Figure 11. The colliding end crush zone is longer than the non-colliding end crush zones and absorbs four times the energy. The total energy absorption capacity provided by the crushable elements in the colliding end was 4,250,000 ft-lbs. (5.76 MJ). The colliding-end crush zone is 5 ft (1.5 m). The crushable elements in the non-colliding end each provided a total energy capacity of 1,062,500 ft-lbs (1.44 MJ). The non-colliding end crush zone is 1.67 ft (0.5 m).

Figure 11: Baseline CEM System Force-Displacement

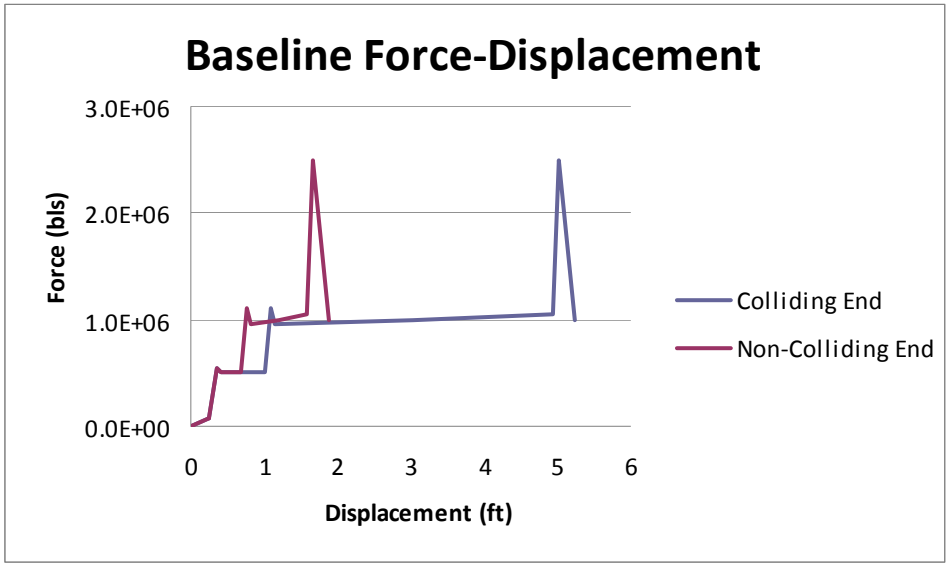

3.1.2. Energy Adjustment

The baseline force-displacement characteristic is used to represent the midpoint of the variables investigated. Energy absorption capacities were adjusted from the baseline condition using two strategies. Each strategy for adjusting the characteristic represents the alternatives available for changing the physical components of the crush zone.

3.1.2.1. Stroke Length Strategy

One way of changing energy capacity is to adjust the length of components. Using this stroke length strategy, the draft gear and pushback coupler features remained the same for every case, only the PEA was adjusted from the baseline. The PEA stroke length was the only characteristic adjusted [Figure 12].

Figure 12: Stroke Length Adjustments

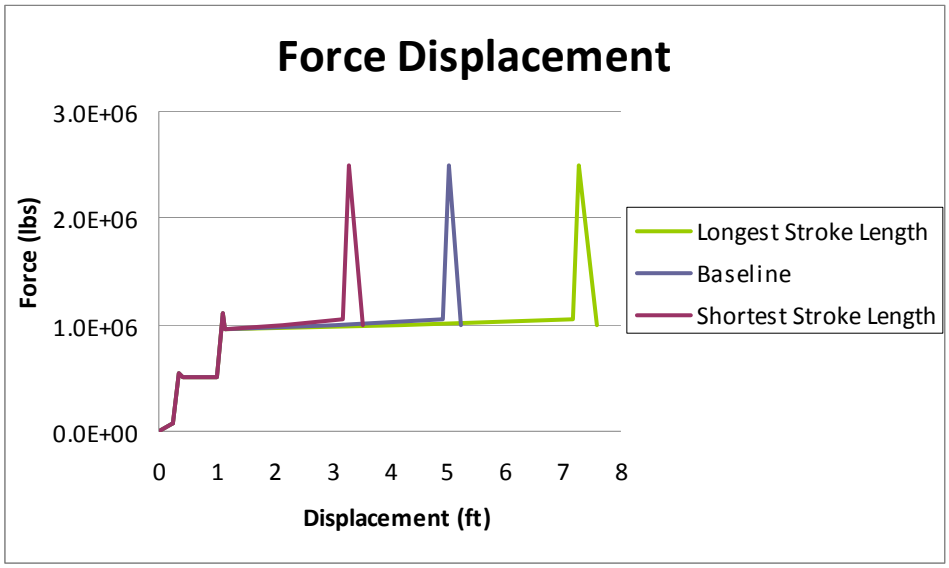

Each adjustment to the colliding end PEA stroke length was made by approximately 1 ft (30 cm) increments. The activation force and all force levels for the colliding-end PEA remained the same. Each 1 ft. adjustment in stroke length corresponds to a 1,000,000 ft lb (1.4 MJ) change in energy absorption capacity. Stroke lengths for the colliding end crush zone varied from approximately 3 ft (91 cm) for the shortest stroke length to 7 ft (2.1 m) for the longest stroke length.

Adjustments to the non-colliding end were made on a smaller scale in order to maintain the same distribution of energy capacity to the colliding and non-colliding ends. Each adjustment to the non-colliding end PEA stroke length was made by approximately 4 in (10 cm) increments. The activation force and all force levels for the non-colliding end PEA

remained the same. Each 4 in. adjustment in stroke length corresponds to a 250,000 ft lb (350 kJ) change in energy absorption capacity.

Table 1 lists the energy capacities that resulted using the stroke length adjustment strategy. The lowest energy absorption capacity is represented by the short crush zone condition. The intermediate short crush zone provides energy capacity falling between the short crush zone and the baseline crush zone. The baseline crush zone represents the midpoint value for crush zone energy capacity. The intermediate long case provides energy capacity falling between the baseline and the long crush one energy capacities. The highest energy absorption capacity is represented by the long crush zone condition.

Table 1: Crush Zone Energy Capacities - Stroke Length Adjustments

Condition	*Colliding End Energy Capacity (ft-lbs)*	*Non-colliding End Energy Capacity (ft-lbs)*	*Trainset Energy Capacity (ft-lbs)*
Short	2,500,000	625,000	6,250,000
Intermediate Short	3,500,000	875,000	8,750,000
Baseline	4,250,000	1,062,000	10,625,000
Intermediate Long	5,500,000	1,375,000	13,750,000
Long	6,500,000	1,625,000	16,250,000

3.1.2.2. Force Level Strategy

Another way of changing energy capacity is to change the strength of components. To represent this, a force level strategy was used for adjusting energy absorption capacity of the baseline characteristic, the draft gear was the only element that remained entirely unaltered. The stroke length for each element remained the same as the baseline for both the colliding and non-colliding ends. The force levels associated with the pushback coupler and primary energy absorber were adjusted [Figure 13].

Figure 13: Force Level Adjustments

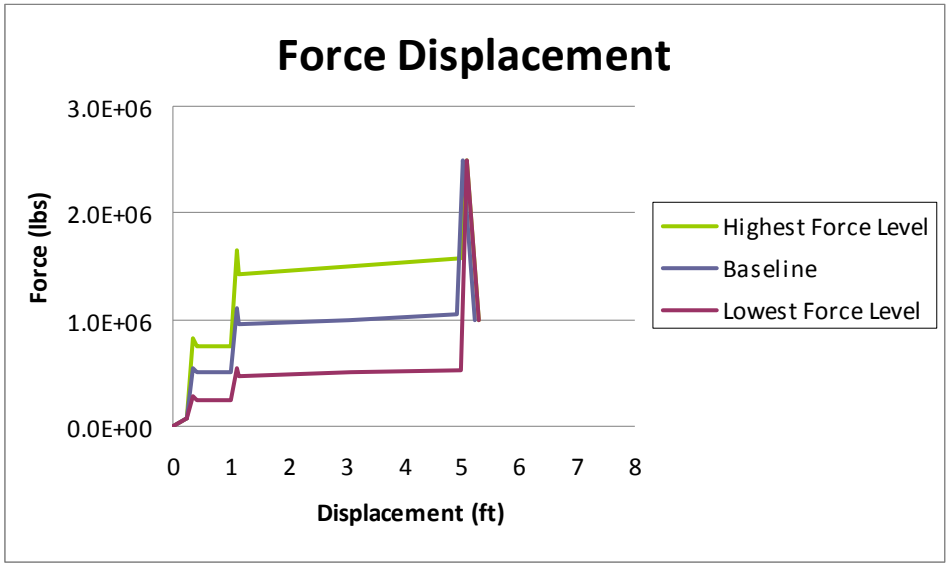

The force level of the pushback coupler was adjusted by 125,000 lb (560 kN) intervals for both the colliding and non-colliding ends. The activation force of the pushback coupler remained 10% higher than the

average force. For the primary energy absorber the average force was adjusted by 250,000 lb (1.1MN) intervals for both the colliding and non-colliding ends. A ± 5% range in force increasing over the length of stroke of the primary energy absorber was maintained. The activation force for the energy absorber was 10% higher than its average force. The PEA force level varied from 5×10^5 lbs (2.2 MN) for the lowest force level to 1.5×10^6 lbs (6.7 MN) for the highest force level.

Unlike the stroke length strategy, alterations were made to multiple components of the crush zone using the force level strategy. Force level adjustments were made to both the pushback coupler and the PEA to maintain the same ratio between their average force levels. The ratio has shown some influence on crush zone collapse and is maintained to eliminate variation in collapse behavior.

Table 2 lists the energy capacities that resulted using the force level adjustment strategy. The lowest energy absorption capacity is represented by the low crush zone condition. The intermediate low crush zone provides energy capacity falling between the short crush zone and the baseline crush zone. The baseline crush zone represents the midpoint value for crush zone energy capacity. The intermediate high case provides energy capacity falling between the baseline and the high crush one energy capacities. The highest energy absorption capacity is represented by the high crush zone condition.

Table 2: Crush Zone Energy Capacities - Force Level Adjustments

Condition	*Colliding End Energy Capacity (ft-lbs)*	*Non-colliding End Energy Capacity (ft-lbs)*	*Trainset Energy Capacity (ft-lbs)*
Low	2,169,000	538,250	5,398,500
Intermediate Low	3,246,500	800,375	8,048,750
Baseline	4,250,000	1,062,500	10,625,000
Intermediate High	5,401,500	1,324,625	13,349,250
High	6,479,000	1,586,750	15,999,500

3.1.3. Crippling Load Adjustment

The crippling load is the peak force on the force-displacement characteristic and represents the maximum force that the occupied volume can support before failure. The allowable deformation of the occupied volume before failure remained the same for all cases. The crippling load is reached after 2.4 in. (6 cm) of deformation of the occupied volume [Figure 14]. The crippling load is adjusted in increments of 1.0 x 10^6 lbs. (4.4 MN) and ranges from 1.5 x 10^6 lbs (6.7 MN) to 3.5 x 10^6 lbs (15.6 MN).

Figure 14: Crippling Load Adjustments

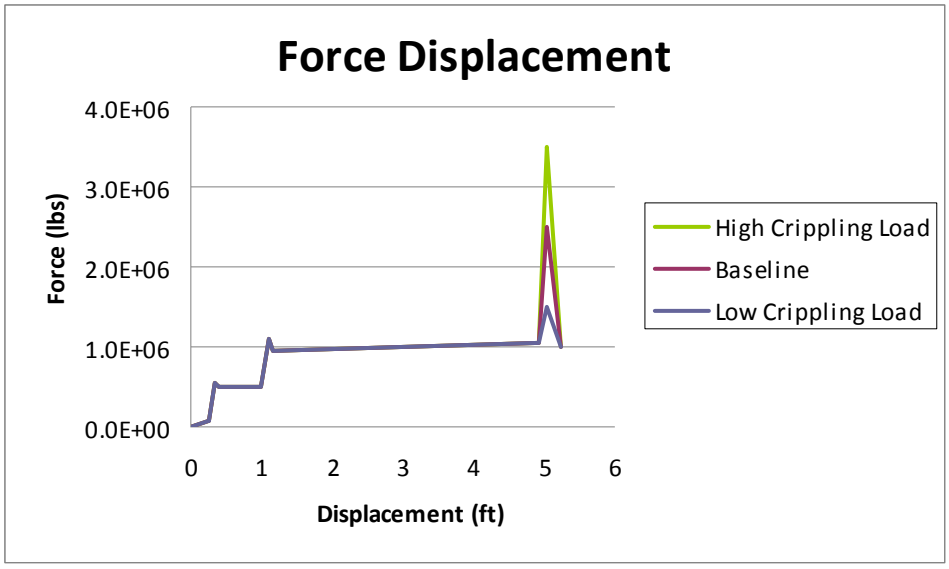

Crippling load values do not directly correspond to buff strength values. The buff strength must be supported without permanent

deformation and occurs in the elastic region of the force-displacement of the occupied volume. The crippling load on the force displacement characteristic describes the maximum force before collapse of the structure. The crippling load defines the maximum force that the structure can support. This value will always be either greater than or equal to the buff strength for static loading conditions and may increase due to dynamic loading conditions.

Each of the 9 unique crush zones included in Table 1 and Table 2 was paired with these three crippling load values. For these cases the crippling load was the same for each car in the trainset. The resulting force-displacement characteristics were reviewed to make sure that they were representative of a functioning system.

One combination of features resulted in a CEM system that would not perform as intended. In this instance, the CEM system had a crippling load weaker than the energy absorbing elements. This would describe a trainset in which the occupied volume would collapse before the energy absorbers. This CEM system would not isolate crush to the allowable areas and maintain space for the passengers to ride out the collision. This case was not analyzed.

In addition to the trainsets comprising cars with the same crippling load, three additional cases are included. For these three cases, the crippling load of the leading car is greater than the crippling load of the trailing cars. The combinations of peak force values are listed in Table 3. These crippling load conditions are paired with the baseline crush zone. The moderate-low condition represents the case where the two lower crippling load values are used, the moderate-high represents the case where the two higher load values are used, and the extreme condition represents the case where the highest and lowest crippling load values are used.

Table 3: Crippling Load Combinations Analyzed

Condition	*Leading Car Crippling load (lbs)*	*Trailing Car Crippling load (lbs)*
Moderate - Low	2,500,000	1,500,000
Moderate - High	3,500,000	2,500,000
Extreme	3,500,000	1,500,000

3.2. Safety Performance Assessment

The safe speed each achieved in the prescribed collision scenario was determined for each trainset. The safe speed is the speed at which crush values do not exceed allowable levels and no occupant volume intrusion occurs. The allowable crush includes the crush zone and the deformation of the occupant volume before the crippling load is reached [Figure 15]. The location of the crippling load on the curve determined the amount of allowable crush for that end. Crush results from the model were compared to the force-displacement characteristic for each end to determine if occupant volume intrusion occurred.

Figure 15: Allowable Crush v. Occupant Volume Intrusion

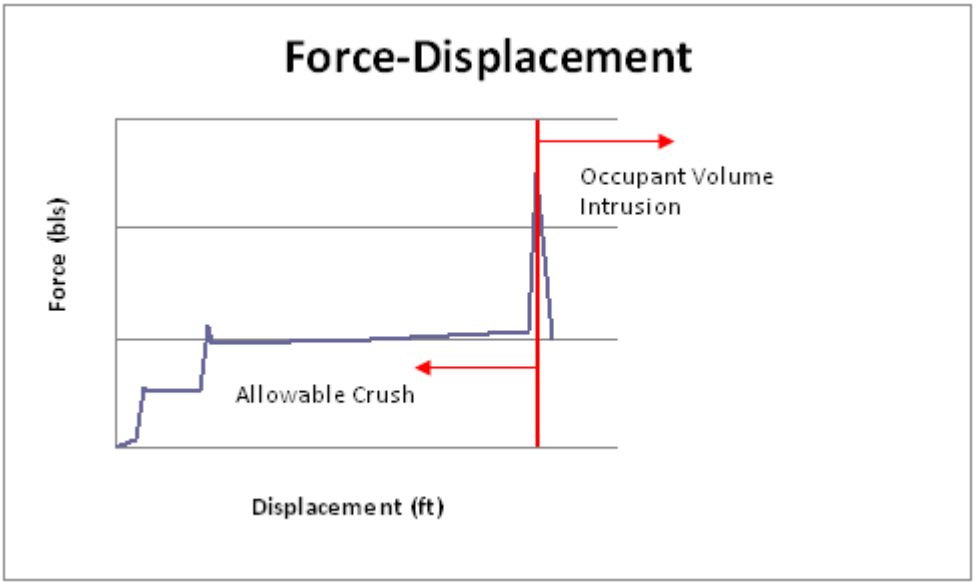

The influence that energy absorption capacity and crippling load magnitude have on passenger safety is further investigated by comparing the secondary impact velocity variations. The secondary impact velocities will be dependent on the collision speed and the characteristics of the CEM system. The SIVs are compared for the extreme values of crush zone stroke length, crush zone force level, and crippling load.

The relative benefits of each energy adjustment strategy are further compared by determining the percentage of utilization for each CEM system. The amount of available energy capacity utilized before occupant volume intrusion occurs is determined for each crush zone design. The effectiveness of each strategy for increasing safe speed is discussed.

4. Results and Discussion

The results of the analysis are examined to determine the influence that the energy absorption capacity and occupant volume integrity have on the crashworthiness. In addition to comparing the effects of energy absorption capacity and level of occupant volume integrity, the influence of strategy used to adjust the energy absorption capacity is also evaluated. The advantages and disadvantages associated with adjusting crush zone length versus adjusting crush zone strength are discussed.

The safe speeds are compared for each adjustment that was made to the CEM characteristics of the trainset. Results are first compared for each energy adjustment strategy while the crippling load remains the same. The effects of altering the crippling load uniformly are then discussed. Finally, the results obtained for trainsets with a stronger leading car will be discussed and compared to the previous results where car strength was uniform for the trainset.

The SIVs are compared for each adjustment that was made to the CEM characteristics of the trainset. These results are compared for each strategy used to adjust the energy capacity of the crush zone and for uniform adjustments to crippling load. The utilization of the CEM systems

are then compared for each strategy used to adjust the energy capacity of the crush zone.

4.1. Safe Speed

The safe speed was determined by running the analysis of the trainset into a rigid wall in 1 mph increments to determine the maximum speed at which allowable crush levels were not exceeded. For the baseline characteristic, the allowable crush at the colliding end is 5.026 ft and at the non-colliding ends is 1.6735 ft. At each of these distances, the crippling load is reached but not exceeded. Figure 16 shows the crush results for the baseline analysis at the safe speed. The crush at each end is shown. End #1 corresponds to the colliding end. At 26 mph, the crush at each end remains at allowable levels. For the analysis of a 27 mph collision, the crush at the colliding end exceeds 5.026 ft and occupant volume intrusion occurs. Thus the safe speed for the baseline case is 26 mph.

Figure 16: Crush Results for the Baseline Case at 26 mph

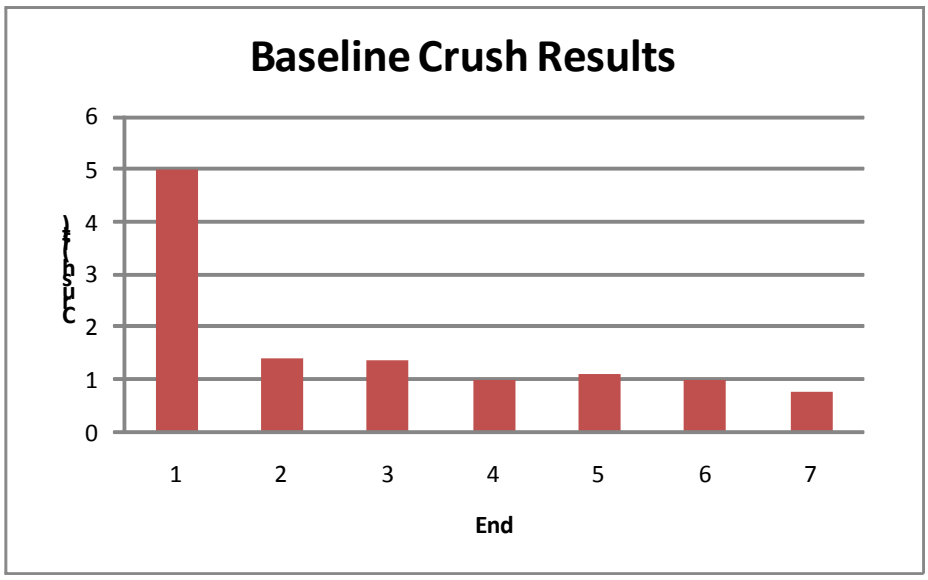

4.1.1. Energy Capacity Adjustment - Stroke Length Strategy

For energy capacities adjusted using the stroke length strategy the allowable crush had to be determined for each case. The allowable crush is determined using the lengths of the crushable elements within the system. Table 4 shows the allowable crush calculated for each end of the trainset for each case. In each case the colliding end has a longer stroke length than the non-colliding ends.

Table 4: Allowable Crush at Each End

Condition	*Allowable Crush at Colliding End (ft)*	*Allowable Crush at Non-Colliding End (ft)*
Short	3.276	1.236
Intermediate Short	4.276	1.486
Baseline	5.026	1.6735
Intermediate Long	6.276	1.986
Long	7.276	2.236

The safe speed results for trainsets adjusted using the stroke length strategy showed that each increase in energy absorption capacity resulted in an increase in safe speed. These results are presented in Figure 17. The baseline result is circled in red in this figure. Safe speeds ranged from 24 mph for the shortest stroke length to 29 mph for the

longest stroke length. In each case, the safe speed was determined when occupant volume intrusion occurred on the colliding end. In some cases there was additional occupant volume intrusion at the non-colliding ends.

Figure 17: Stroke Length Adjustment Strategy

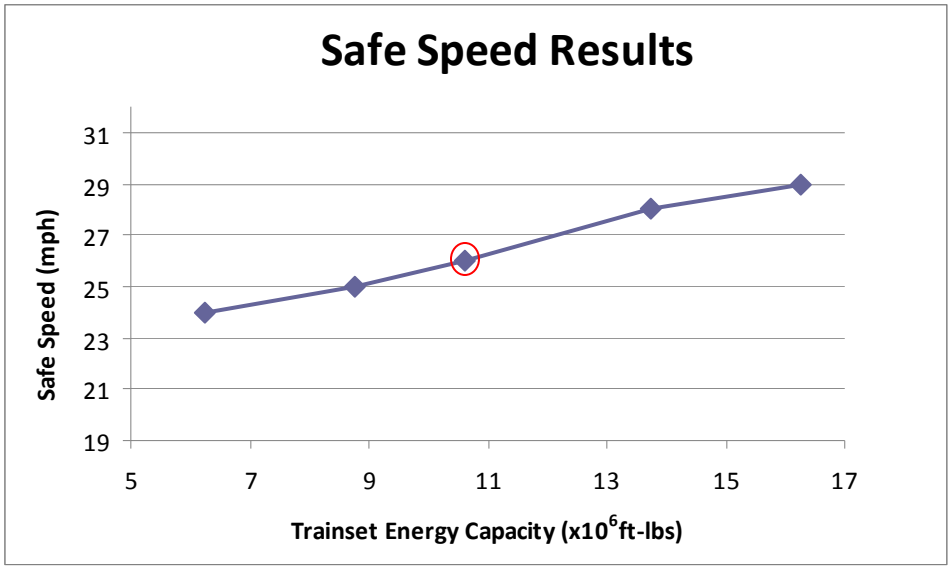

4.1.2. Energy Capacity Adjustment - Force Level Strategy

For cases adjusted using the force level strategy, the allowable crush remained the same for each case. The allowable crush at the colliding end is 5.026 ft and at each non-colliding end is 1.6735 ft; the same values as the baseline case.

Using the force level strategy, each incremental increase in energy absorption capacity showed a corresponding increase in safe speed.

These results are presented in Figure 18. The baseline result is included for comparison and is circled in red. The safe speed ranged from 20 mph for the lowest force level to 31 mph for the highest force level. In each case occupant volume intrusion occurred on the colliding end, determining the safe speed.

Figure 18: Force Level Adjustment Strategy

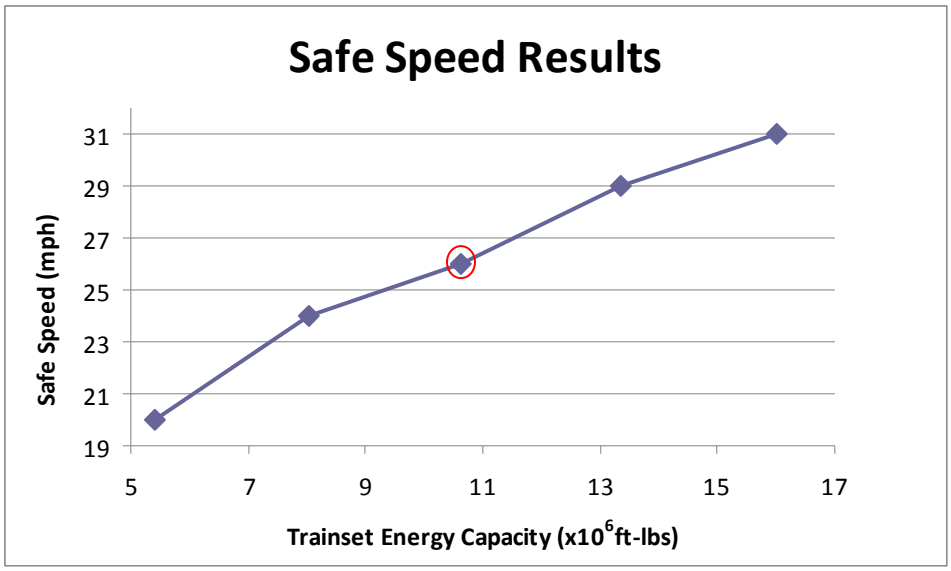

4.1.3. Crippling Load Adjustments – Cars of Equal Strength

Increasing the energy absorption capacity of the CEM system increased the safe speed achieved in a collision with a wall. However, the energy absorption capacity is only one portion of the CEM system. The effect of varying the crippling load of the occupied volume was also

examined. The crippling load was varied by the same amount for each vehicle in the trainset.

For crippling load adjustments made to a force-displacement characteristic with the baseline energy capacity, each 1 x 10^6 lb change in crippling load resulted in a 1 mph change in safe speed. Figure 19 shows the safe speed for each of these cases. The baseline result is circled in red in the figure. The safe speed for the lowest crippling load was 25 mph and the safe speed for the highest crippling load was 27 mph. The crippling loads examined ranged from 1.5 x 10^6 lbs to 3.5 x 10^6 lbs.

Figure 19: Crippling Load Adjustments to Baseline Energy Capacity

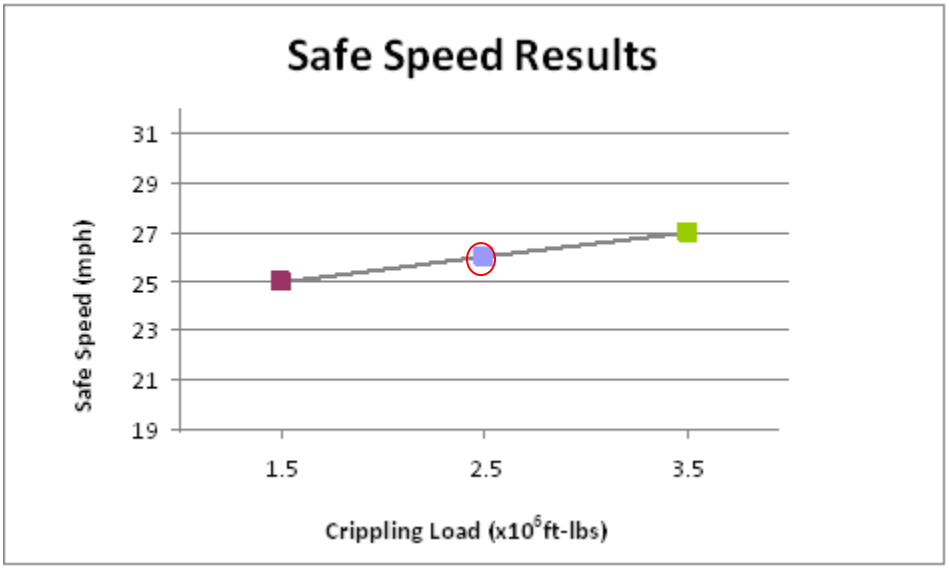

Each crippling load magnitude was paired with each of the energy capacities adjusted using the stroke length strategy. The safe speeds for

this set of analyses are presented in Figure 20. Each line in the figure represents a different crippling load value. The safe speed for the baseline case, which comprises the baseline energy capacity and baseline crippling load, is circled in red. The lines show that for a given crippling load, increasing the energy capacity of the CEM system results in an increase in safe speed. By comparing the safe speed values for a given energy capacity, it can be seen that increases in crippling load only resulted in an increase in safe speed in some cases.

Figure 20: Variations in Crippling Load and Stroke Length

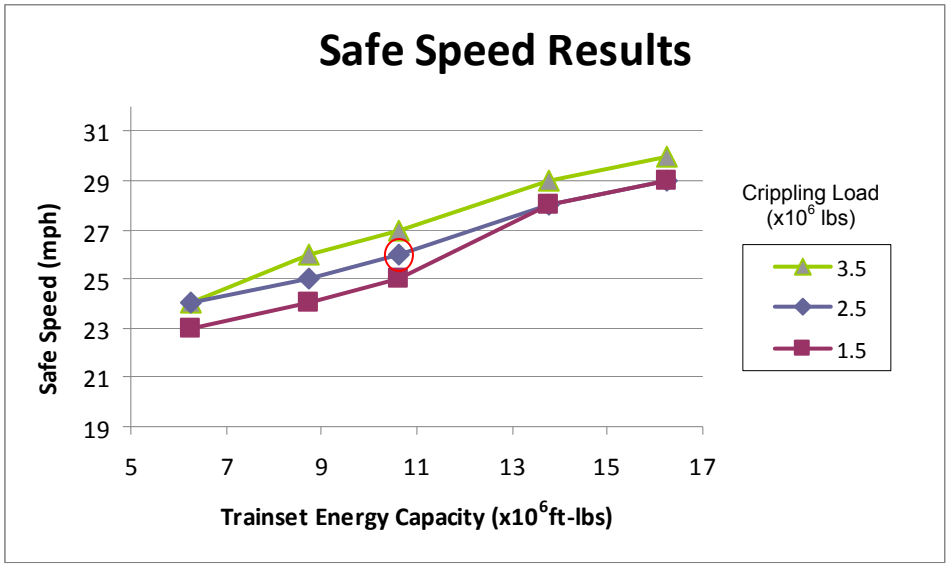

Each crippling load magnitude was then paired with the energy capacities adjusted using the force level strategy. The combination of the highest energy absorption capacity and the lowest crippling load value

was not physically realistic. This case was not be analyzed. As a result, only two crippling load magnitudes were paired with the highest energy absorber force level. The safe speed results of these analyses are presented in Figure 21. Each line in the figure represents a different crippling load value. The safe speed for the baseline case is again circled in red.

Figure 21: Variations in Crippling Load and Energy Absorber Force Level

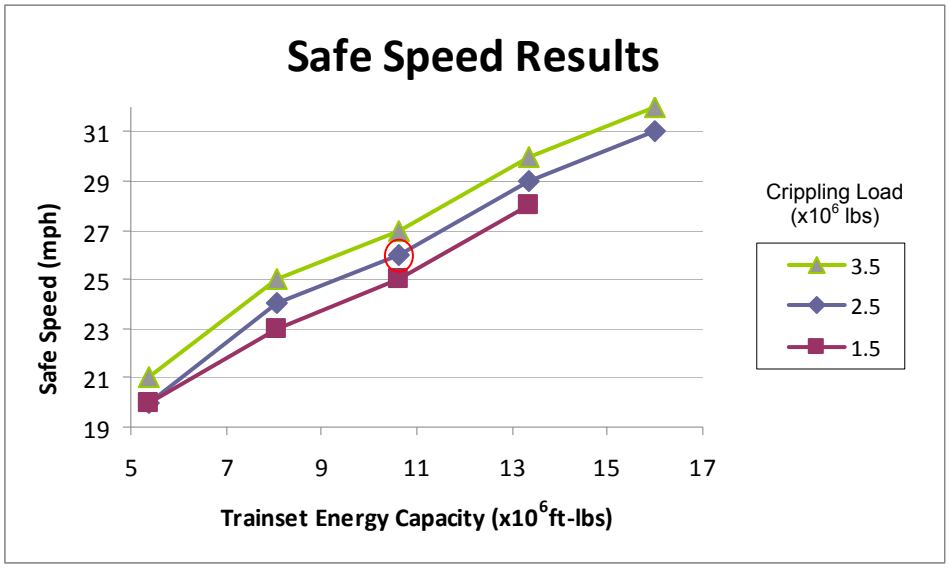

The results indicate that for a given crippling load magnitude, increasing the energy capacity of the CEM system results in an increase in safe speed. Comparing the safe speed results for a given energy capacity shows that increases in crippling load resulted in an increase in safe speed in most cases. For the lowest energy absorption capacity,

increasing the crippling load from 1.5 x 10^6 lb to 2.5 x 10^6 lb had no effect on safe speed.

4.1.4. Crippling Load Adjustments – Stronger Leading Car

To further investigate the influence of crippling load, an additional strategy employed cars of different strength in the same consist. In these cases the leading car crippling load was greater than the trailing car crippling load. Using the baseline crush zone characteristic, the effect of increasing only the leading car crippling load was examined. The safe speed results from this strategy are presented in Table 5. The previous results from uniform crippling load adjustments made to the baseline crush zone are included for comparison. The baseline case safe speed is presented in bold.

Table 5: Safe Speed Results

Safe Speed (mph)				
		Leading Car Crippling load (x 10^6 lb)		
		3.5	2.5	1.5
Trailing Car Crippling load (x 10^6 lb)	3.5	27		
	2.5	27	**26**	
	1.5	26	26	25

For the two cases with a leading car crippling load 1 x 10^6 lbs greater than the trailing cars, occupant volume intrusion occurred at the colliding end. In these cases the crippling load of the trailing cars did not

influence the safe speed in the range examined. The safe speed results are consistent with the previously analyzed cases of the same colliding end crush zone and crippling load magnitude.

For the case with a leading car crippling load 2 x 10^6 lbs greater than the trailing cars, the crippling load of the trailing cars did influence the safe speed. In this case occupant volume intrusion occurred at the third end rather than at the colliding end. The safe speed is lower than the previously analyzed case of the same colliding end crush zone and crippling magnitude of 3.5 x 10^6 lbs.

4.1.5. Safe Speed Summary

Comparing the safe speed results for each adjustment, it can be seen that increasing either the energy absorption capacity or the crippling load increases the safe speed in most cases. Increasing the energy absorption capacity allows for more collision energy to be safely absorbed and controlled by the system. Increasing the crippling load increases the forces that the occupied volume can withstand before it crushes.

In this series of analyses, increasing the energy absorption capacity of the trainset while maintaining the same crippling load magnitude resulted in an increase in safe speed in all cases. Increasing the crippling load for

a given energy capacity did not always result in an increase in safe speed however. In each case where the crippling load was adjusted uniformly for each car in the trainset, crush occurred at all interfaces and the safe speed was determined when crush values exceeded allowable levels at the colliding end.

For the cases where the leading car was stronger than the trailing cars, this increased strength was seen to increase the safe speed up to a point. Increasing the strength of the leading vehicle prevented crushing of the leading vehicle. The trailing cars however, must still be strong enough to withstand the forces transferred to them in the collision. In one case the leading car withstood the collision without loss of occupied volume while a trailing car failed.

4.2. SIV

The safe speed is one result for evaluating crashworthiness. Once it has been determined that there is space for the occupants to survive the collision the forces that the occupants are subjected to must be considered. The severity of these forces will determine if increasing the safe speed was effective at improving the overall crashworthiness of the system. As the speed of the collision increases, the forces acting on the occupants also have the potential to increase.

The forces acting on the occupants can be described by determining the SIV characteristic of each vehicle in the trainset. The SIV is the relative velocity of the occupant with respect to the interior of the train as the vehicles decelerate. In collisions at speeds greater than 20 mph the interior environment may present a concern. Since all of the safe speeds determined in this research were above 20 mph, the secondary impact velocity for each case indicates a potentially threatening environment.

The SIV is calculated for the baseline case and shown in Figure 22. The SIV characteristic represents the velocity of an unrestrained passenger in free flight. The displacements represent the distance that the passenger travels before striking the interior of the occupant volume and can correspond to various seating arrangements. Displacements of less than 1ft. are associated with rear-facing seats. Displacements of less than 2 ft. are associated with passengers seated at tables that restrict passenger movement during a collision. Displacements of 3 ft or less are associated with passengers seated in rows of forward-facing seats.

Figure 22: Relative Acceleration of Passengers within the Trainset

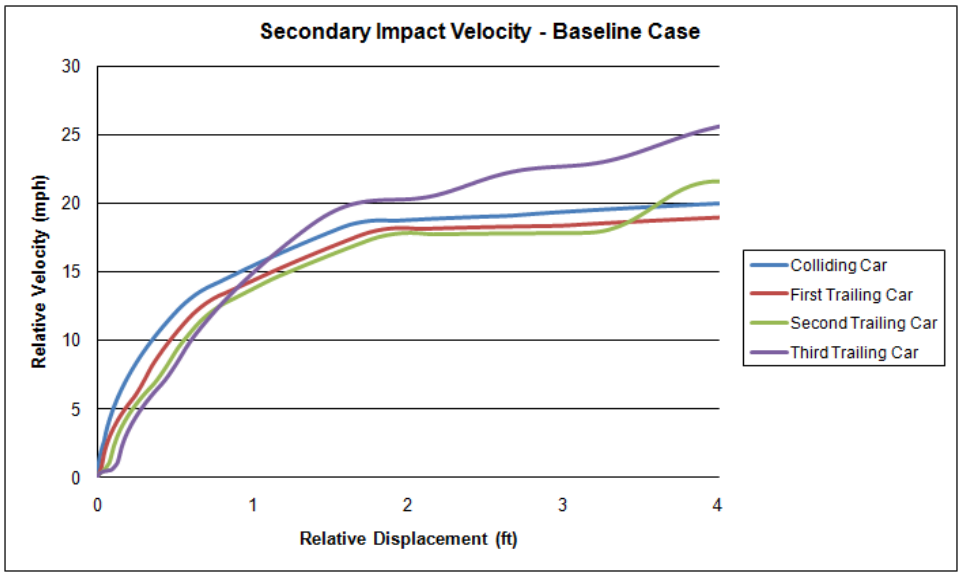

The particular design features of a CEM system can affect the way the car decelerates and may be capable of mitigating the severity of the occupant environment. In order to examine how each adjustment strategy influences the SIV, the decelerations of each car were determined for adjustments made to the energy absorbing elements of the CEM system. The SIV characteristic is determined for a collision at the safe speed. The highest SIV at a displacement of 3 ft is compared.

4.2.1. SIV Results – Stroke Length Strategy

Increases to the stroke length showed a decrease in SIV at a relative displacement of 3 ft. Figure 23 shows the safe speed and the SIV for the baseline and extreme cases of energy capacity adjusted using the stroke

length strategy. The SIV is determined for a collision at the safe speed. The SIV for the shortest crush zone was 27 mph and was reduced to 22 mph for the longest crush zone. Even as collision speeds increased, the SIV was less severe for the longer crush zones. Increasing the stroke length indicates a more gradual deceleration of the trainset.

Figure 23: SIV Results at 3 ft – Stroke Length Adjustments

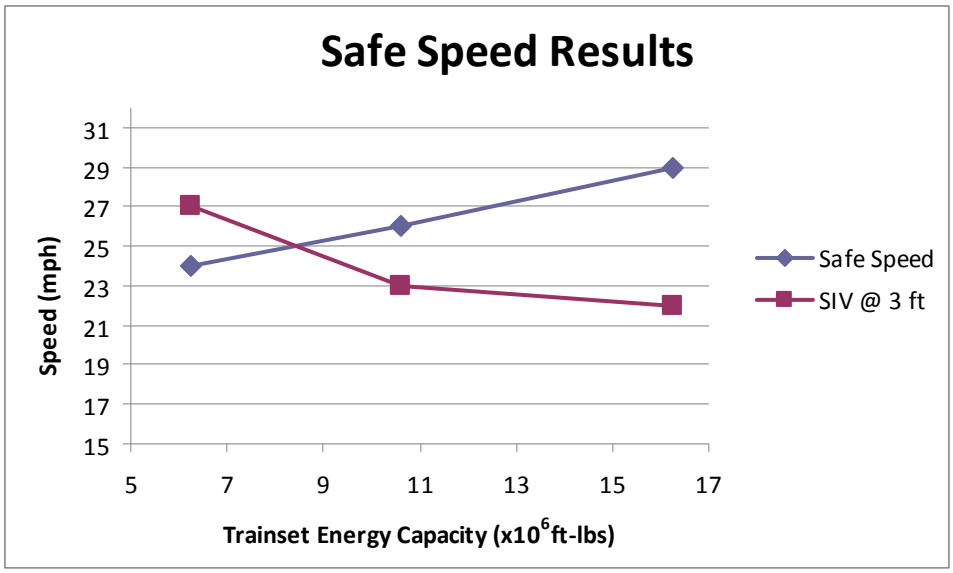

4.2.2. SIV Results – Force Level Strategy

As the crush zone force levels increased, the SIV at 3 ft of relative displacement also increased for collisions at the safe speed. Figure 24 shows the safe speed and the SIV for the baseline and extreme cases of energy capacity adjusted using the force level strategy. The SIV is determined for a collision at the safe speed. The SIV for the lowest force

level was 17 mph and increased to 27 mph for the highest force level. This increase in SIV corresponded to the increase in collision speed. For each force level, the SIV at 3 ft was 3 mph less than the safe speed.

Figure 24: SIV Results at 3 ft –Force Level Adjustments

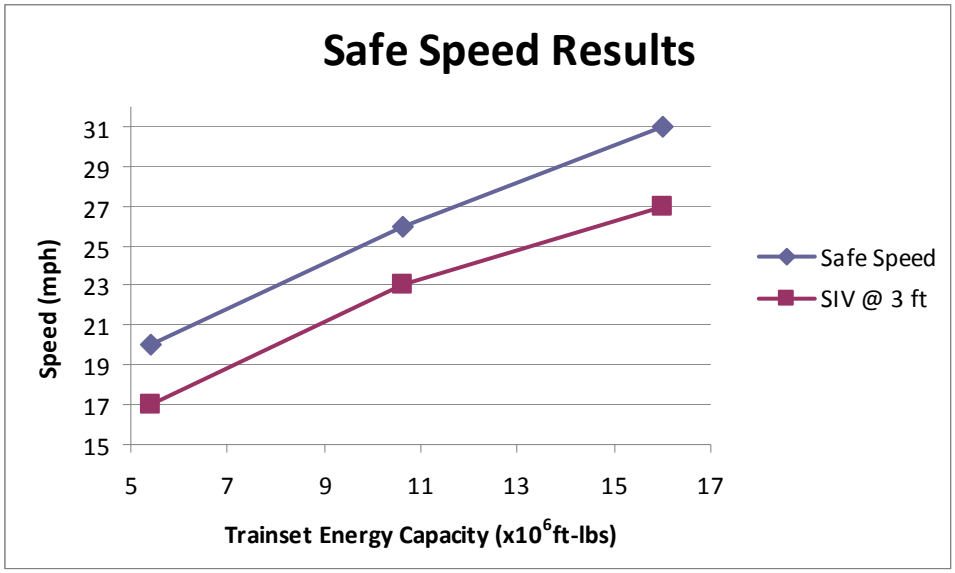

4.2.3. SIV Summary

The crippling load values do not affect the severity of the deceleration, and therefore do not affect the SIV. The strategy used to adjust the energy absorption capacity will influence the severity of the deceleration. Increasing the stroke length of the crush zone will reduce the severity of the SIV while increasing the safe speed. Longer crush ones allow for more gradual deceleration of the trainset. Increasing the force levels of

the crush zone increases the SIV. The SIV increases at the same rate that the safe speed increases.

4.3. CEM Utilization

In order to further compare the relative benefits of the strategy used to adjust the energy capacity of the CEM system, the utilization of available energy capacity was examined for each case. Effective utilization of crush zones is a concern for systems where weight and space are limited resources. The percentage of utilization is evaluated by comparing the total available energy capacity of the CEM system to the amount of collision energy absorbed at the safe speed. 100% utilization would indicate a collision in which the entire energy capacity of the system is exhausted without occupied volume intrusion.

The utilization of the CEM system is determined at the safe speed. In each case the colliding end crush zone is utilized completely and the percentage of utilization determines how much energy is absorbed by trailing interfaces. Once occupant volume intrusion occurs, the collision energy can no longer be limited to the crush zones, and crush becomes uncontrolled. The energy absorbed at the safe speed is the maximum amount of energy that is safely managed by the CEM system.

The percentages of utilization were compared for each of the nine energy capacities for a system with a crippling load of 2.5 x 10^6 lbs. For the baseline case, the CEM system uses 67% of its total capacity for the collision at the safe speed. The colliding end has exhausted the energy capacity of the crushable elements and begun utilizing the additional energy capacity provided by the allowable deformation of the occupant volume. The non-colliding ends are not yet exhausted [Figure 25]. For collisions at higher speeds, the colliding end's occupied volume will begin crushing without utilizing any of the remaining available capacity in the non-colliding ends.

Figure 25: Baseline System Energy Utilized at Safe Speed

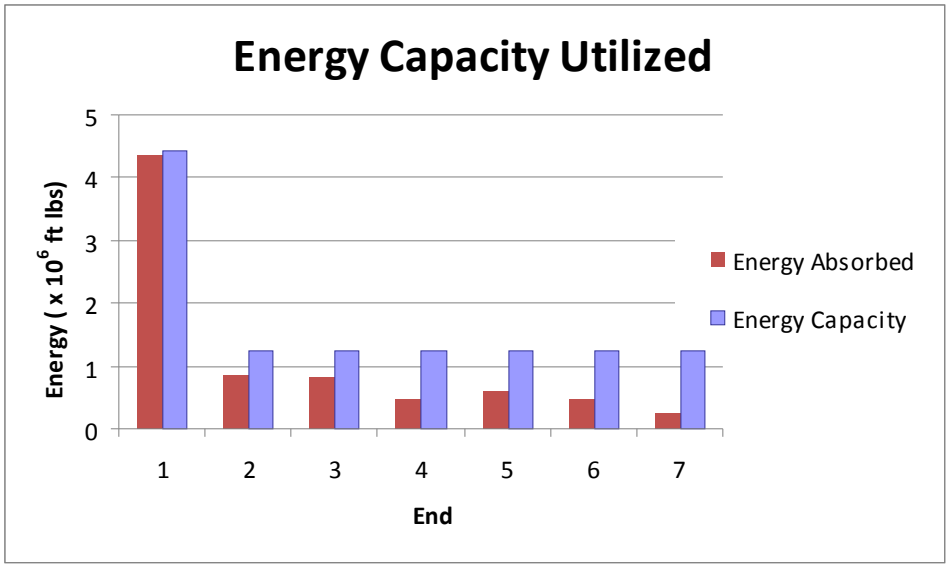

4.3.1. Energy Utilization – Stroke Length Strategy

When the energy capacity is adjusted using the stroke length strategy, the utilization of the CEM system also changes. Figure 26 shows the percentage of utilization for each energy capacity adjusted using the stroke length strategy. The baseline value is circled in red. As the stroke length increases the utilization of the system decreases. For the shortest stroke length, the CEM system safely utilizes 91% of its available capacity to manage the collision energy. For the longest stroke length, the system is able to safely utilize only 56% of the available energy capacity at the highest speed without occupant volume intrusion.

Figure 26: CEM Utilization – Stroke Length Adjustment Strategy

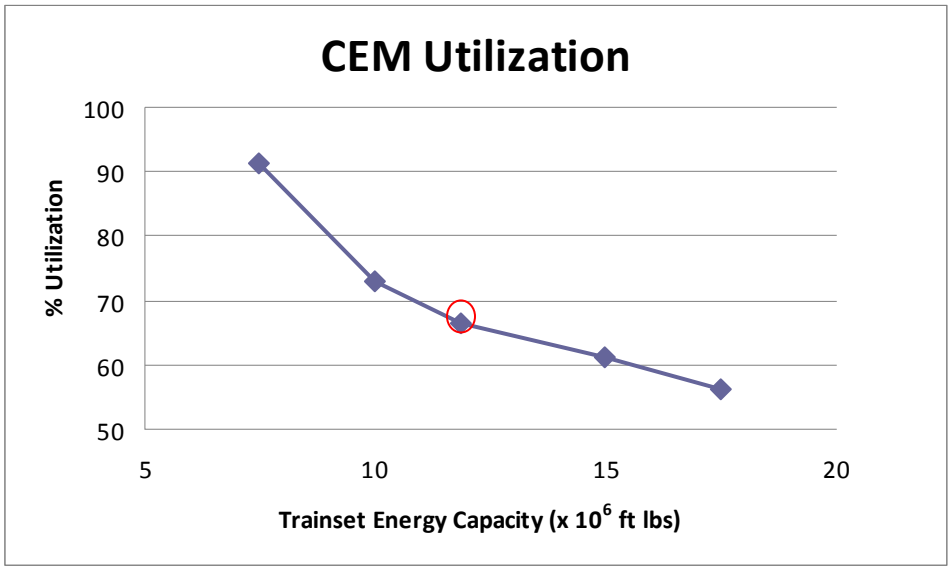

4.3.2. Energy Utilization– Force Level Strategy

Force level adjustments do not appear to affect the utilization of the system as dramatically as stroke length adjustments. Figure 27 shows the percentage of utilization for each energy capacity adjusted using the force level strategy. The baseline value is circled in red. For the lowest average force level, the CEM system safely utilizes 69% of its available capacity to manage the collision energy at the safe speed. For the highest average force level, the system is able to utilize 66% of the available energy capacity at the safe speed.

Figure 27: CEM Utilization – Force Level Adjustment Strategy

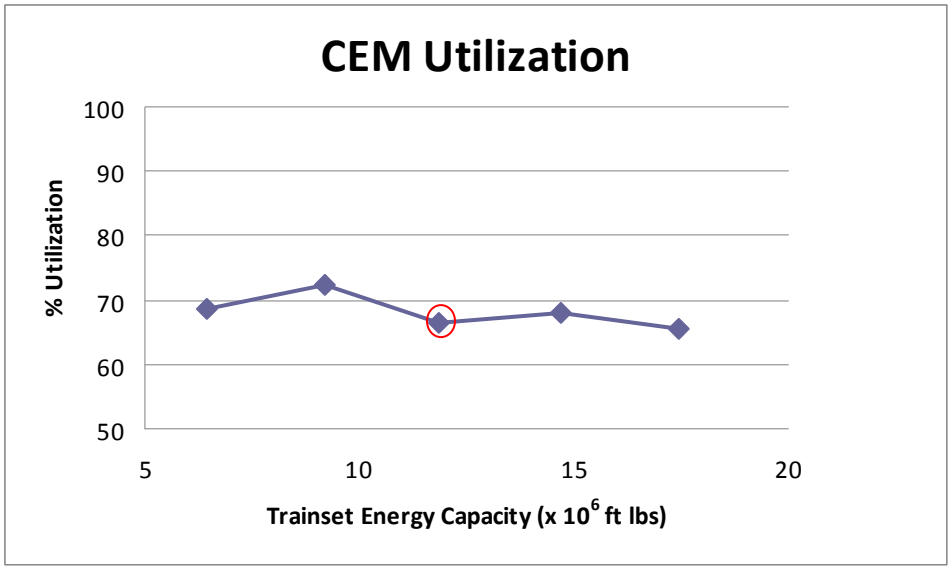

4.3.3. Utilization Summary

Increasing the energy capacity of the system using either strategy increased the safe speed of the trainset. The effectiveness of this increase was dependent on the method. Figure 28 shows the rate of increase in safe speed when energy capacity is added for both methods. Making the crush zone longer increased the available energy absorption capacity, but reduced the utilization of the system at the safe speed. Making the crush zone stronger increased the energy absorption capacity while maintaining the same utilization at the safe speed. Energy capacity added to the system by increasing force levels was more effective at increasing safe speed than energy capacity added by increasing the stroke length.

Figure 28: Safe Speed Results – Strategy Comparison

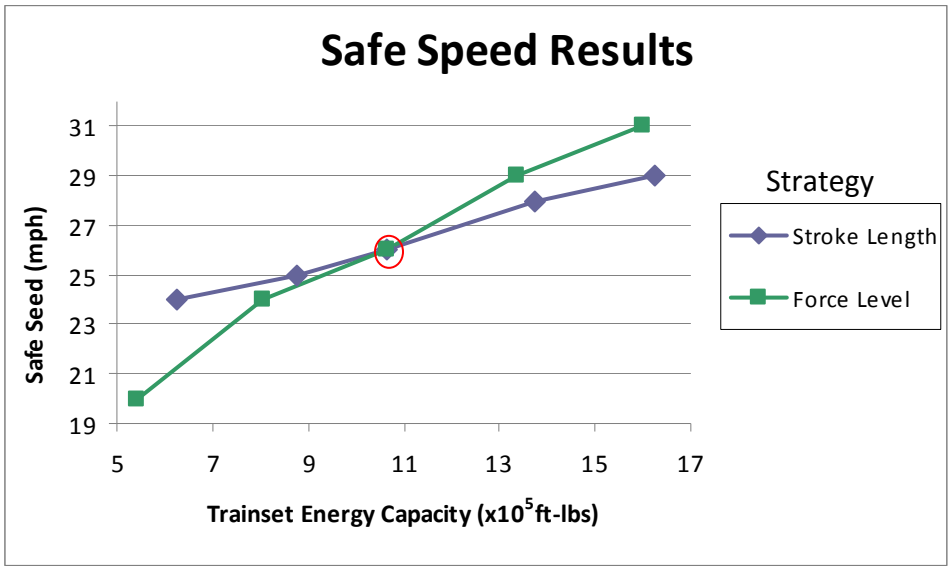

5. Summary

The goal of this thesis was to explore high speed rail systems and determine the level of structural crashworthiness provided. A survey of high-speed systems was performed. The primary component of structural crashworthiness for high speed equipment is a CEM system. A collision dynamics model was constructed to represent these high speed vehicles. The model included parameters that were easily varied, in particular the energy absorption capacity and occupant volume strength features of the CEM system. An appropriate collision scenario was selected after reviewing accidents involving high speed equipment. The model was then executed for various CEM system configurations.

The results of the collision scenario analyses determined the influence that the energy absorption capacity and occupant volume integrity have on the crashworthiness. Adjustments to the occupant volume integrity were made by adjusting the crippling load of the structure. Adjustments to the energy absorption capacity of the crush zone were made by either increasing the length or the strength of the crushable elements. The results of safe speed and SIV were used to compare the effects of varying the energy absorption capacity and occupant volume integrity. The strategies used to adjust the energy absorption capacity were compared using the results of safe speed, SIV, and utilization of the CEM system.

The safe speed of the trainset was determined for each adjustment made to the trainset. Increasing either the energy absorption capacity or crippling load increases the safe speed in most cases. Increasing the energy absorption capacity allows for more collision energy to be safely absorbed and controlled by the system. Increasing the crippling load magnitude increases the forces that the occupied volume can withstand before it crushes. For each configuration examined with cars of equal strength, crush occurred at all interfaces throughout the train and the safe speed was determined when occupant volume intrusion occurred at the colliding end.

A series of collisions was examined where the leading car had a higher crippling load magnitude than the trailing cars. For the cases where the leading car was stronger than the trailing cars, this increased strength was able to increase the safe speed, but only up to a point. Increasing the strength of the leading vehicle prevents crushing of the leading vehicle where conditions are the most critical. Even with this increased crippling load, the trailing cars however must still be strong enough to withstand the forces transferred to them in the collision.

The influence that energy adjustment strategy and crippling load have on passenger safety was further investigated by comparing the secondary

impact velocity fluctuations. The severity of the secondary impact velocity is affected by the strategy used to adjust the energy absorption capacity. Increasing the stroke length of the crush zone will reduce the severity of the SIV with respect to the safe speed. Longer crush zones allow for more gradual deceleration of the trainset. Increasing the force levels of the crush zone increases the SIV, but only as the safe speed increases.

The relative benefits of each energy adjustment strategy are further compared by determining the utilization of each CEM system configuration. Making the crush zone longer increases the available energy absorption capacity, but reduces the utilization of the system. Making the crush zone stronger increases the energy absorption capacity while maintaining the same level of utilization. Adding energy capacity to the system by increasing force levels was more effective at increasing safe speed than adding energy capacity by increasing the stroke length.

6. Conclusions

The goal of this thesis was to explore high speed systems and determine the level of structural crashworthiness provided by high speed rail systems. For many high speed systems, structural crashworthiness is provided by a CEM system. Two main features of the CEM system are the energy absorbing crush zone and the occupant volume. By determining the influence of these CEM components, inferences were made about how the crashworthiness high speed equipment could be improved.

Each of the operating high speed systems is capable of providing an acceptable level of crashworthiness for the environment in which is operates. This is determined by the ability of the equipment to meet safety requirements for operation. In order to expand operation to more varied environments, it may be required to increase the level of crashworthiness. In order to achieve this, improvements can be made to the major components of the CEM system.

Increasing the magnitude of the crippling load is one option for increasing safe speed. This would require large-scale improvements to the structure of the carbody however. If the market for expansion is large, it may be worth producing a large number of vehicles with a stronger

occupied volume. It may also be possible to increase the strength of the leading car only. In this case it would be necessary to demonstrate that this does not present a hazard to trailing cars in the trainset.

Increasing the energy absorption capacity of the crush zone is another option for increasing safe speed. Adjustments to the crush zone may be more desirable due to the localized nature of these changes, but the residual effects on SIV and utilization must be considered. For situations where space is limited or weight is a concern, increasing the force level of the crush zone elements is a good option. Energy capacity added in this manner will not increase the space devoted to the crush zone, and can be more effective at increasing the safe speed. The effect this has on SIV may be a concern if changes cannot be made to the interior to mitigate the effects of collision forces. It is also important to consider the complexity of the crush zone. Force level adjustments may need to be made to multiple elements to maintain the gradual increase in force levels supported by the crush zone, as this plays a role in controlling collision forces.

For situations where the SIV or the extent of improvements is a concern, increasing the stroke length of the crush zone may be the best option. The SIV can be reduced by increasing the stroke length of the crush zone. This can be achieved by increasing the stroke length of the

primary energy absorbing feature only. Increasing the stroke length will require additional space however, and the energy capacity added will not be as effectively utilized towards increasing the safe speed.

Each adjustment to the CEM system has its own advantages and disadvantages. These must be weighed by the engineer for each existing equipment design and the intended application. It is possible to increase the level of safety that a crashworthy structure can provide by making localized adjustments, but it is also important to determine how these adjustments affect the function of the whole system. A well-designed CEM system is one that relies on each feature to work together to provide passenger safety.

Appendix 1: Force-Displacement Characteristics of Vehicle Structures

In a full-scale test, the vehicle response can be measured for the collision. This is typically done by using accelerometers. Accelerometer data can be used to determine the forces on the vehicle when multiplied by the mass, and integrated to determine the velocity and displacement. In this way, the high frequency noise is filtered and a force-displacement approximation of the vehicle response can be obtained. The force-displacement approximation, shown in Figure 29, is a more convenient way of defining the vehicle behavior for a collision dynamics analysis.

Figure 29: Example Force Displacement Collision Dynamics Input

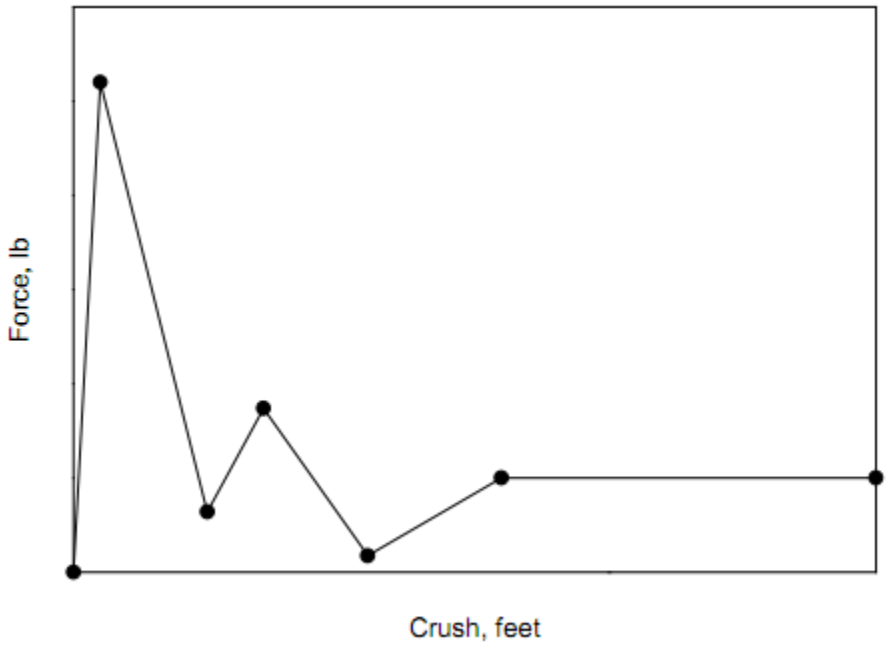

The force-displacement characteristic is a simplified input for a spring-mass collision dynamics analysis. Adjustments can be made easily to describe a variety of equipment. The force crush characteristic is a good approximation of the response of the vehicle in a collision. Using the collision dynamics analysis, a time-acceleration result can be obtained for the vehicle in the collision. This analysis agrees with the results obtained in full-scale testing.

Figure 30: Example Acceleration for Vehicle CG in a collision

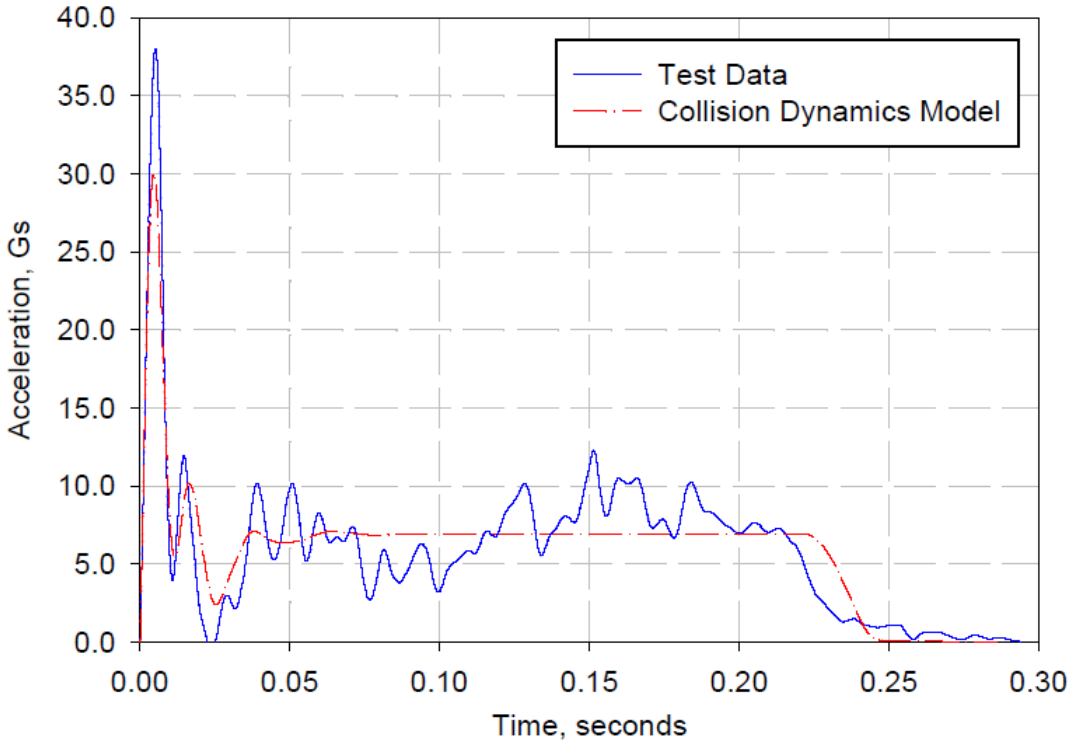

In the simplest form, the forces acting upon the vehicle structure can be represented by a spring-mass system [Figure 31]. The spring represents the deformation characteristics of the vehicle end being loaded. The spring characteristics will determine how much the spring deforms and the forces that get transferred to the rigid mass.

Figure 31: Force Applied to a Spring-Mass system

This approximation of a rigid mass with a deformable spring characteristic captures the deformable nature of the vehicle structures. While the vehicle is largely a rigid body, there are areas of deformation when large forces are applied. This type of analysis is valid when deformation is limited or in the case of a CEM system, where deformation is controlled. The rigid mass represents the strong occupied volume, and the deformable spring represents the crush zone.

The spring-mass system not only works for static loads, but for dynamic loading conditions as well. The system can be expanded to represent a series of vehicles [Figure 32]; including not only the behavior of a single vehicle, but the interaction between vehicles as well. The analysis now accounts for the timing of the collision as the deformation wave passes through the train. The first spring compresses before the rigid body is able to transfer load to the next spring. The vehicle interaction can be represented by a composite force displacement characteristic that accounts for both interfaces, or single-end characteristics can be modeled in series.

Figure 32: Force Applied to an Expanded Spring-Mass System

Unlike a linear spring, which can be defined by a single stiffness value, the force-displacement characteristic of a vehicle structure is non linear. The complexity of the structure can lead to multiple stages of behavior. Figure 33 illustrates two features of varying stiffness that crush in series. The initial force is relatively low, but as the structure is compressed further, the stiffness increases. This compression is not elastic; as the structure is unloaded an additional behavior is observed. Some of the displacement will be recovered, and some is permanent.

Figure 33: Relative Force Displacement Behavior

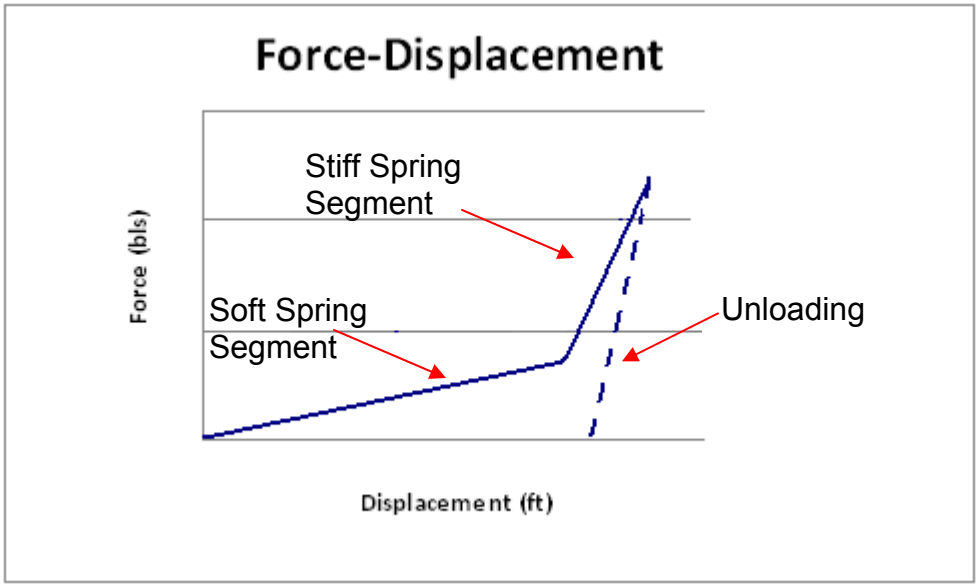

For a CEM system, the crush zone can be represented by the soft spring segment. In practice this structure will not be a single feature with a linear crush characteristic, but may comprise multiple elements. Multiple stages can be used to gradually increase the force level of the crush zone [Figure 34]. The gradual increase in force level allows for progressive crush of the structure while limiting severe decelerations of the vehicle. The size and shape of these stages will determine the deceleration of the trainset.

Figure 34: Increasing Stages of the Crush Zone

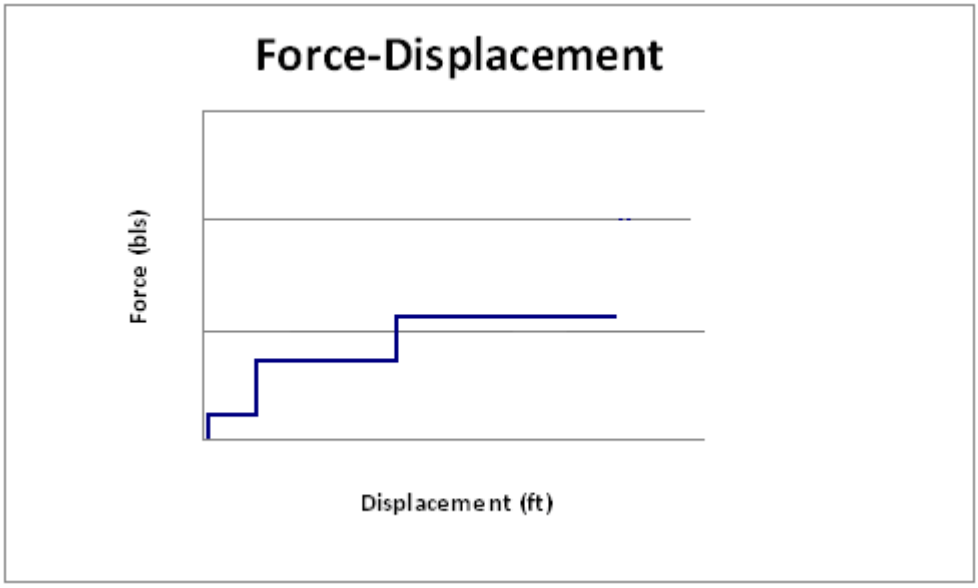

Each stage has an average force and a displacement associated with it. This displacement is also called a stroke length. As stages transition from a low force stage to a high force stage, in particular in a dynamic loading situation, the force level may experience overshoot at activation [Figure 35]. This peak exists while crush is triggered and drops to the force level of the stage as crushing proceeds.

Figure 35: Activation Force

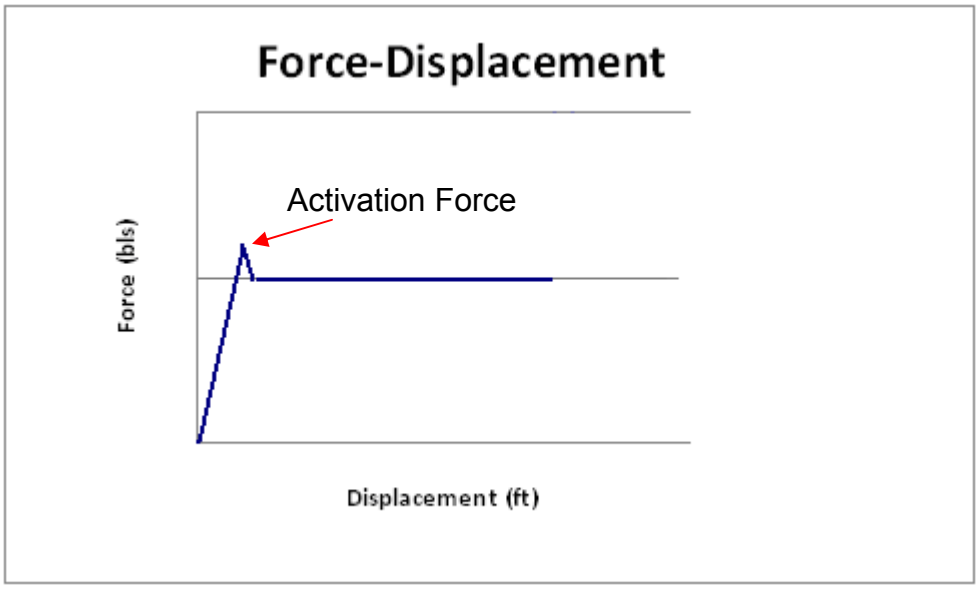

The activation force should be slight enough that it does not prevent crushing of the stage. In some cases crushing can be promoted by slightly lowering the force level after initiation. In order to maintain the same average force, the force levels are slightly increased at exhaustion. This creates a slight slope in force level over the stroke length [Figure 36].

Figure 36: Sloped Force Level

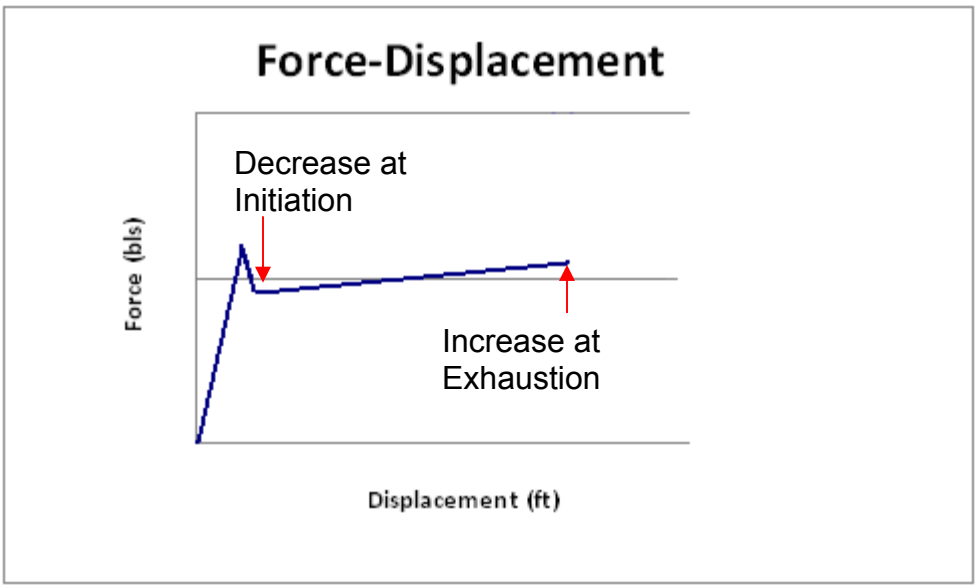

The continuous gradual increase in force level facilitates controlled crushing of the structure. In some designs there may be gaps between stages during crushing. No force is supported by the structure while the gap is being closed. This discontinuity does not interfere with crushing if the force level after the drop out is at least as high as the force level supported before drop out [Figure 37].

Figure 37: Drop out in Force

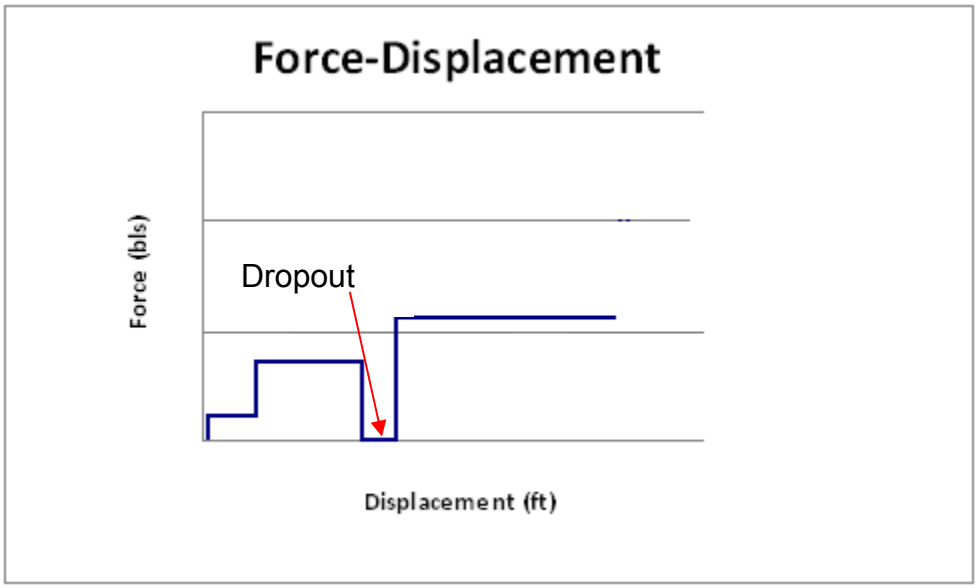

As the crush zones deform, they absorb kinetic energy. The energy absorbed by the system is represented by the area under the curve [Figure 38]. The level of force and the length of stroke determine the energy capacity of each stage. This means that increasing the energy absorption capacity of the CEM system occurs when the force levels are increased or the stroke levels are increased. The force levels will affect the severity of the deceleration and increasing the stroke length uses space. Alterations to either of these characteristics must be made while keeping the effects in mind.

Figure 38: Energy Absorbed by the Crush Zone

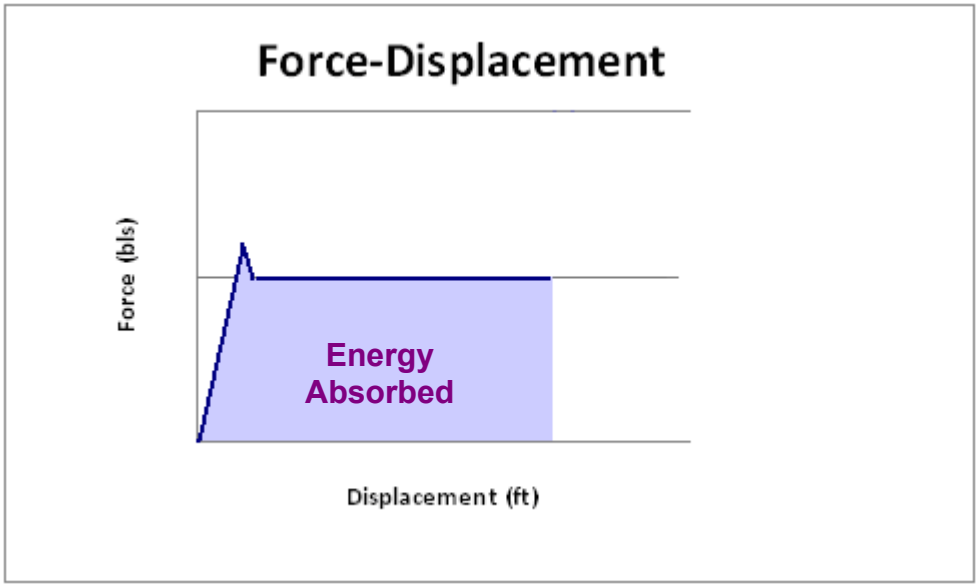

The stages of the force-displacement characteristic correspond to the components of the crush zone. A more detailed description of how a system of crushable components can be represented by a force-

displacement characteristic can be found in Appendix 3. In general, standard components such as the draft gear and coupler are included, as well as any additional features. These components must be able to support service loads without damage. For example, the coupler must remain functional during operation and through a hard shunt. Once force levels exceed these, as in a collision, the coupler can be designed to deform and absorb collision energy. The pushback coupler is capable of supporting a level of force while it crushes to exhaustion [Figure 39].

Figure 39: Draft Gear and Coupler Schematics

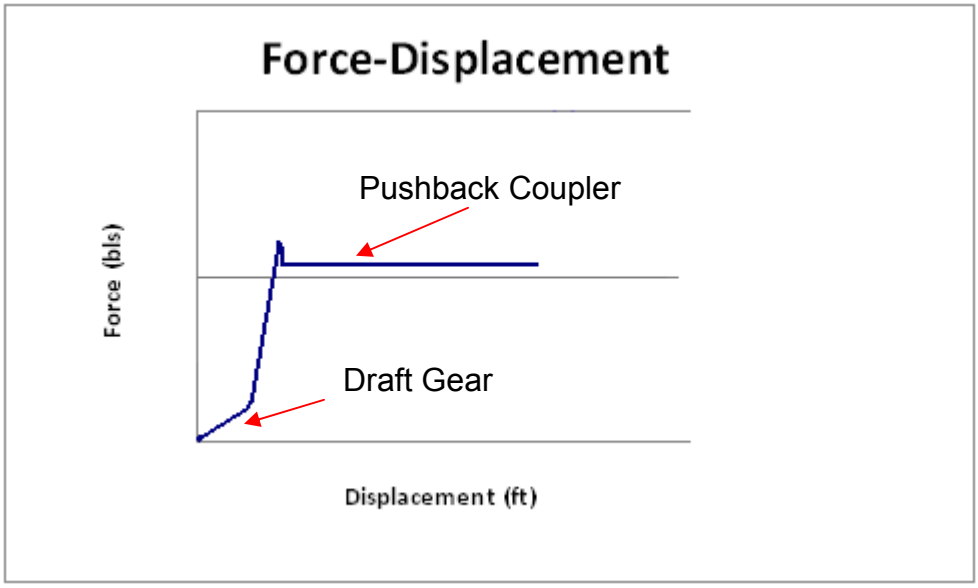

In some cases energy absorbers may also be added to the system to absorb energy after the pushback coupler has been exhausted [Figure 40]. Energy absorbers can be constructed out of multiple deformable materials such as honeycomb structures and deformable tubes. Shear bolts can be used to control breakaway features, and notches can be utilized to control regions of material failure.

Figure 40: Components of the Crush Zone

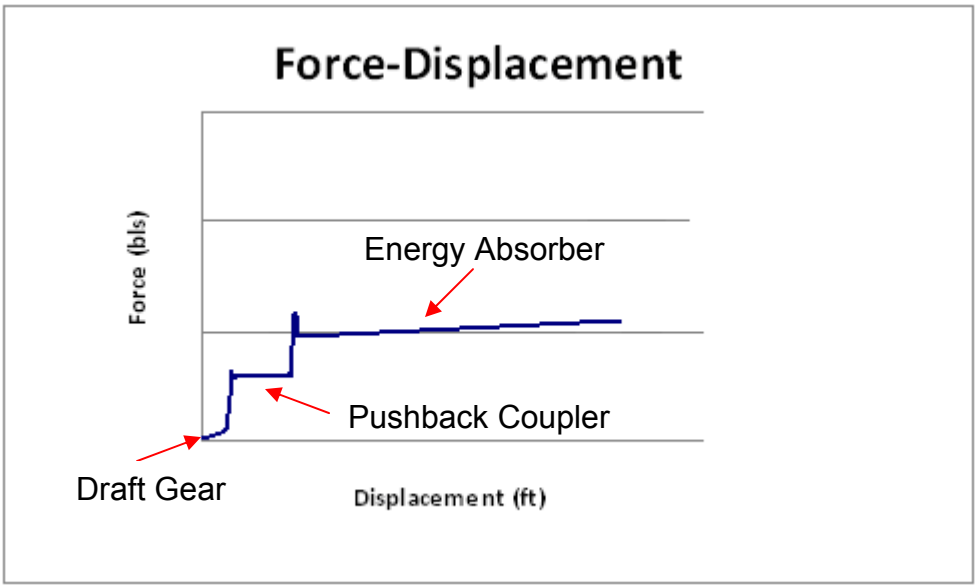

The occupied volume is the final stage of the system [Figure 41]. The force crush characteristic for the occupied volume is comparatively stiff. The deformation of the occupied volume before the crippling load is reached will provide some additional energy absorption. The crippling load defines the maximum force supported by the structure and once it

has been exceeded the occupied area begins to crush. Once this occurs the system ceases to function as intended.

Figure 41: The Crush Zone and Occupied Volume

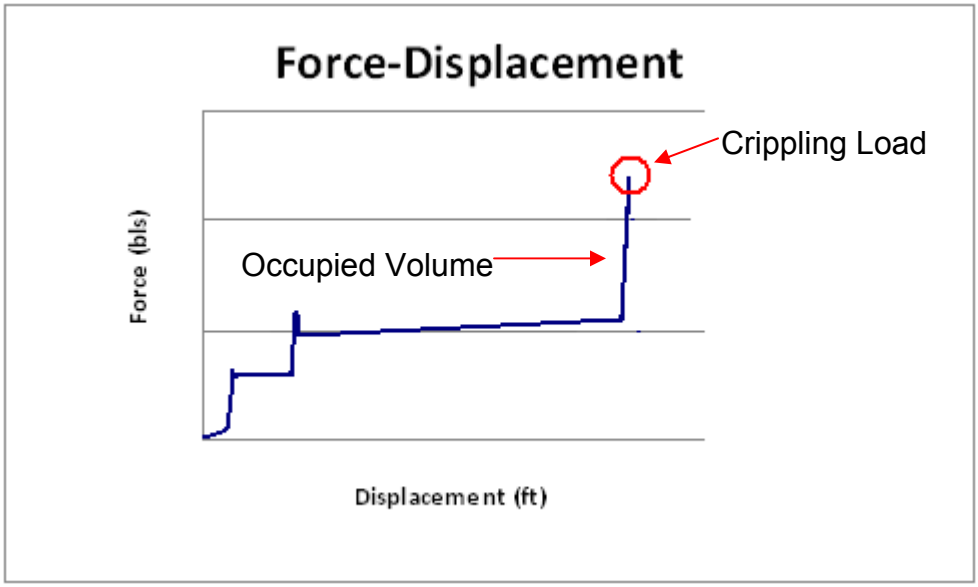

There are some practical limits to the characteristics of the CEM system. The force levels associated with the crush zone are limited by the materials utilized in the crush zone and the peak force of the occupied volume. The weight and size of each feature must be carefully considered before addition into the system. There is a limited amount of space available to maximize both crush zone length and occupant capacity.

Appendix 2: CEM Equipment Survey

This survey compiles information on CEM equipment, both high speed and conventional speeds. Details are provided as available. Equipment is arranged alphabetically. This information is intended to provide a snapshot of what high speed systems exist and where they operate. In addition to providing general information, details on trainset configuration, collision energy capacity and buff strength requirements will contribute to model characteristics that will be used for analysis.

The country of installment and the years of operation provide information on the operating environment. The presence of train control systems, the maintenance of the infrastructure, and any additional traffic will all play a role in the overall safety of the system. The age of the equipment gives a general idea of the technology available at the time and the system for which the equipment was designed.

The location of operation will also narrow down what safety regulations apply to the equipment. For example, it is assumed that equipment operating in Europe will meet the EuroNorm requirements in effect at the time of installment [25]. Safety regulations may include operational requirements, structural requirements or occupant protections features. Each country has developed these requirements over time to

respond to the operating environment and focus may be put on different qualities.

Buff strength requirements are included as a point of comparison. They do not directly correlate to the occupant volume integrity. Buff strength requirements are the forces that must be met without permanent deformation. The occupant volume integrity is represented by the crippling load, the maximum force before failure, of the structure. The crippling load will always be either greater than or equal to the buff strength for static loading conditions.

The collision energy capacity discussed is the capacity of designated crush zones. In many cases the vehicle shell will be capable of absorbing energy as it deforms before failure of the structure. These additional energy absorbing capabilities of the equipment have not been accounted for.

High Speed Equipment

Acela

- Manufacturer: Bombardier/Alstom
- Configuration: Locomotive – transition car – 4 passenger cars – transition car – locomotive
- Country of Installment: USA
- Operator: Amtrak
- Years of Service: 2000-present
- Maximum Speed: 150 mph
- Train Weight: 1230 kips
- Passenger Capacity: 345
- Collision Energy Capacity: Figure 2 illustrates the CEM capacity at each interface of the power cars, transition cars, and passenger cars.
- Buff Strength Requirement: See Figure 2

AGV [26, 27, 28]

- Manufacturer: Alstom
- Configuration: 7-14 car articulated EMU
- Country of Installment: Italy
- Operator: Nuovo Trasporto Viaggiatori, (NTV)
- Years of Service: Not yet in operation

- Maximum Speed: 225 mph
- Train Weight: 820 kips (11-car trainset)
- Passenger Capacity: 250-650
- Collision Energy Capacity: 3.5 x 10^6 ft-lbs (4.8 MJ) at colliding ends
- Buff Strength Requirement: 337 kips

AVE S-102 [29, 30]

- Manufacturer: Talgo, Bombardier
- Configuration: Traction Unit – 12 passenger cars – Traction Unit
- Country of Installment: Spain
- Operator: RENFE
- Years of Service: 2005 - Present
- Maximum Speed: 205 mph
- Train Weight: 720 kips
- Passenger Capacity: 318
- Collision Energy Capacity: Unknown
- Buff Strength Requirement: 450 kips

ICE 2 [31]

- Manufacturer: Siemens, Bombardier
- Configuration: Power head - 6 intermediate coaches – Power head
- Country of Installment: Germany
- Operator: Deutsche Bahn (DB)

- Years of Service: 1995-present
- Maximum Speed: 174 mph
- Train Weight: 904 kips
- Passenger Capacity: 389
- Collision Energy Capacity: Unknown
- Buff Strength Requirement: 450 kips

ICE 3 [32]

- Manufacturer: Siemens, Bombardier
- Configuration: 8-car EMU
- Country of Installment: Germany, The Netherlands
- Operator: DB, Nederlandse Spoorwegen (NS)
- Years of Service: 2000-present
- Maximum Speed: 205 mph
- Train Weight: 818 kips
- Passenger Capacity: 441
- Collision Energy Capacity: Unknown
- Buff Strength Requirement: 337 kips

Talgo 250 [33]

- Manufacturer: Talgo
- Configuration: Traction Unit – 11 passenger cars – Traction Unit
- Country of Installment: Spain

- Operator: RENFE
- Years of Service: 2009 - Present
- Maximum Speed: 155 mph
- Train Weight: 720 kips
- Passenger Capacity: 265 -289
- Collision Energy Capacity: Unknown
- Buff Strength Requirement: 450 kips

TGV-R [34 , 18]

- Manufacturer: Alstom
- Configuration: Power car - 8 intermediate passenger cars – power car
- Country of Installment: France
- Operator: SNCF, Thalys
- Years of Service: 1992-present
- Maximum Speed: 186 mph
- Train Weight: 850 kips
- Passenger Capacity: 377
- Collision Energy Capacity: None
- Buff Strength Requirement: 450 kips

TGV Duplex [18, 35]

- Manufacturer: Alstom
- Configuration: power car – transition car - 6 intermediate passenger cars – transition car - power car
- Country of Installment: France
- Operator: SNCF
- Years of Service: 1995-present
- Maximum Speed: 186 mph
- Train Weight: 838 kips
- Passenger Capacity: 545
- Collision Energy Capacity: Figure 1 illustrates the CEM capacity at each interface of the power cars, transition cars, and passenger cars.
- Buff Strength Requirement: 450 kips

Shinkansen N700-I [36]

- Manufacturer: Nippon Sharyo
- Configuration: 6 – 16 car EMU
- Country of Installment: Japan
- Operator: JR Central, JR West
- Years of Service: 2007 - present
- Maximum Speed: 205 mph
- Train Weight: 805 kips (8 car)

- Passenger Capacity: 636 (8 car)
- Collision Energy Capacity: None
- Buff Strength Requirement: Not available

V250 [37,45]

- Manufacturer: Ansaldo Breda
- Configuration: 8-car EMU
- Country of Installment: Belgium, The Netherlands
- Operator: SNCB, NS
- Years of Service: Not yet in operation
- Maximum Speed: 155 mph
- Train Weight: 970 kips
- Passenger Capacity: 546
- Collision Energy Capacity: 4.3×10^6 ft-lbs (5.8 MJ) at colliding end, 6.5×10^5 ft-lbs (0.88 MJ) at non-colliding ends
- Buff Strength Requirement: 337 kips

Velaro [38, 39, 40]

- Manufacturer: Siemens
- Configuration: 8-10 car EMU
- Country of Installment: China, Russia
- Operator: China MOR, Russian Railways (RZD)
- Years of Service: 2007 - present

- Maximum Speed: 186 mph
- Train Weight: 850 kips (8-car trainset)
- Passenger Capacity: 600
- Collision Energy Capacity: 2.2 x 10^6 ft-lbs (3 MJ) at colliding ends, 4.4 x 10^5 ft-lbs (0.6 MJ) at non-colliding ends
- Buff Strength Requirement: 337 kips

Zefiro V300 [45, 41]

- Manufacturer: Ansaldo Breda, Bombardier
- Configuration: 8-car or 16-car EMU
- Country of Installment: Italy
- Operator:
- Years of Service: Not yet in operation
- Maximum Speed: 225 mph
- Train Weight: 892 kips (8 car)
- Passenger Capacity: 600 (8 car)
- Collision Energy Capacity: 2.2 x 10^6 ft-lbs (3 MJ) absorbed in cab car
- Buff Strength Requirement: 337 kips

Zefiro 380 [41]

- Manufacturer: Bombardier
- Configuration: 8-car or 16-car EMU

- Country of Installment: China
- Operator: China MOR
- Years of Service: Not yet in Operation
- Maximum Speed: 240 mph
- Train Weight: 942 kips (8 car)
- Passenger Capacity: 495 (8 car)
- Collision Energy Capacity: 1.5 – 3.0 x 10^6 ft-lb (2 – 4 MJ) adjustable at colliding end, energy absorbing pushback couplers at non-colliding ends
- Buff Strength Requirement: 337 kips

Conventional Speed CEM Equipment

Coradia 1000 [16, 42]

- Manufacturer: Alstom
- Configuration: 5-car DMU
- Country of Installment: United Kingdom
- Operator: British Rail
- Years of Service: 2002 - present
- Maximum Speed: 125 mph
- Train Weight: 557 kips
- Passenger Capacity: 287

- Collision Energy Capacity: 2.2 x 10^6 ft lb (3.0 MJ) for the colliding end, 7.8 x 10^5 ft lb (1.06 MJ) for intermediate ends
- Buff Strength Requirement: 450 kips

Flirt NSB [43]

- Manufacturer: Stadler
- Configuration: 5-car EMU
- Country of Installment: Norway
- Operator: Norges Statsbaner
- Years of Service: Not yet in Operation
- Maximum Speed: 125 mph
- Train Weight: 474 kips
- Passenger Capacity: 264
- Collision Energy Capacity: 2.0 x 10^6 ft lb (2.7 MJ) on colliding ends
- Buff Strength Requirement: 337 kips

Metrolink [44]

- Manufacturer: Hyundai Rotem
- Configuration: Locomotive – 2 passenger cars – cab car
- Country of Installment: United States
- Operator: Southern California Regional Rail Authority (SCRRA)
- Years of Service: 2010 - Present

- Maximum Speed: 110 mph
- Train Weight: 720 kips
- Passenger Capacity: 392
- Collision Energy Capacity: 3.5 x 10^6 ft lb (4.7 MJ) cab car colliding end, 2.6 x 10^6 ft lb (3.5 MJ) cab car trailing end, 3 x 10^5 ft lb (0.4 MJ) on passenger car ends
- Buff Strength Requirement: 800 kips

A summary of the high-speed equipment survey are presented in Table 6 and Table 7. Trainset configurations vary between distributed power trainsets and power car-led trainsets. A majority of the trainsets are not articulated. The trainset length provided in the table is the length associated with the weight provided in the table. In many cases multiple configurations exist of the same type of equipment.

Table 6: Summary of High Speed Equipment Composition

Train	Max. Speed (mph)	Power Car / Distributed Power	Coupling	Trainset Length (cars)	Trainset Weight (kips)
Acela	150	Power Car	Non-Articulated	8	1230
AGV	225	Distributed Power	Articulated	11	820
AVE S-102	205	Power Car	Non-Articulated	14	720
ICE 2	174	Power Car	Non-Articulated	8	904
ICE 3	205	Distributed Power	Non-Articulated	8	818
Talgo 250	155	Power Car	Non-Articulated	13	720
TGV- R	186	Power Car	Articulated	10	850
TGV Duplex	186	Power Car	Articulated	10	838
N700-I	205	Distributed Power	Non-Articulated	8	805
V250	155	Distributed Power	Non-Articulated	8	970
Velaro	186	Distributed Power	Non-Articulated	8	850
Zefiro 300	225	Distributed Power	Non-Articulated	8	892
Zefiro 380	240	Distributed Power	Non-Articulated	8	942

Table 7 provides a Summary of the CEM information associated with each high-speed trainset. For equipment incorporating a CEM system, the total energy absorption capacity of the trainset ranges from 3 x 10^6 ft-lbs absorbed at the colliding ends of the Zefiro 380 to 3.4 x 10^7 ft-lbs absorbed at multiple crush zones on the Acela. Buff strength

requirements range from 337 kips for the current TSI HS requirement for P-II to 2100 kips for a CFR tier II Locomotive.

Table 7: Summary of High Speed Equipment CEM information

Train	Max. Speed (mph)	Weight per car (kips)	Total Trainset Energy Capacity (MJ)	Energy Capacity of first 4 cars (MJ)	Min. Compressive Force (kips)
Acela	150	154	46	21	800 / 1200 / 2100
AGV	225	75	9.6	4.8	337*
AVE S-102	205	51	--		450†
ICE 2	174	113	--		450†
ICE 3	205	102	--		337*
Talgo 250	155	55	--		450†
TGV- R	186	85	0		450†
TGV Duplex	186	84	29.2	12.2	1100 / 900
N700-I	205	101	0		--
V250	155	121	23.92	11.08	337*
Velaro	186	106	14.4	6.6	337*
Zefiro 300	225	111	6	3	337*
Zefiro 380	240	118	4 - 8	2 - 4	337*

*Equipment assumed to be in compliance with TSI HS requirement for P-II

†Equipment assumed to be in compliance with TSI HS requirement for P-I

Appendix 3: Force – Displacement Approximations

The crush zone itself may comprise multiple elements. The force displacement characteristic is refined to describe its composition. Each feature can be represented by a portion of the force-displacement curve. The force-displacement characteristic is the short story of how the crush zone is assembled.

Draft gears and couplers are generally standard equipment for North American operational purposes. Multiple energy absorbers may be included in the crush zone. The primary energy absorber absorbs the bulk of the collision energy. Additional energy absorbers can be used to control lateral displacements. Energy absorbing anti-climbers can prevent the system from overriding. Figure 42 shows an example of a crush zone with multiple energy absorbers.

Figure 42: Example Colliding End CEM System

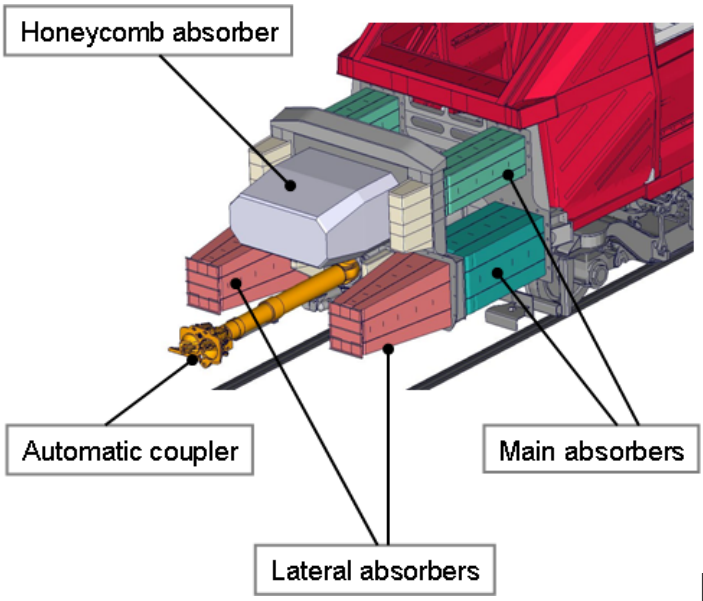

[45]

The force-displacement information for these elements are then assembled into a single schematic. Figure 43 illustrates how the properties of each element of the system can be assembled to describe the longitudinal behavior of the CEM system. The size and location of each element in relation to each other is accounted for.

Figure 43: Example Force-Displacement Schematic for a CEM system

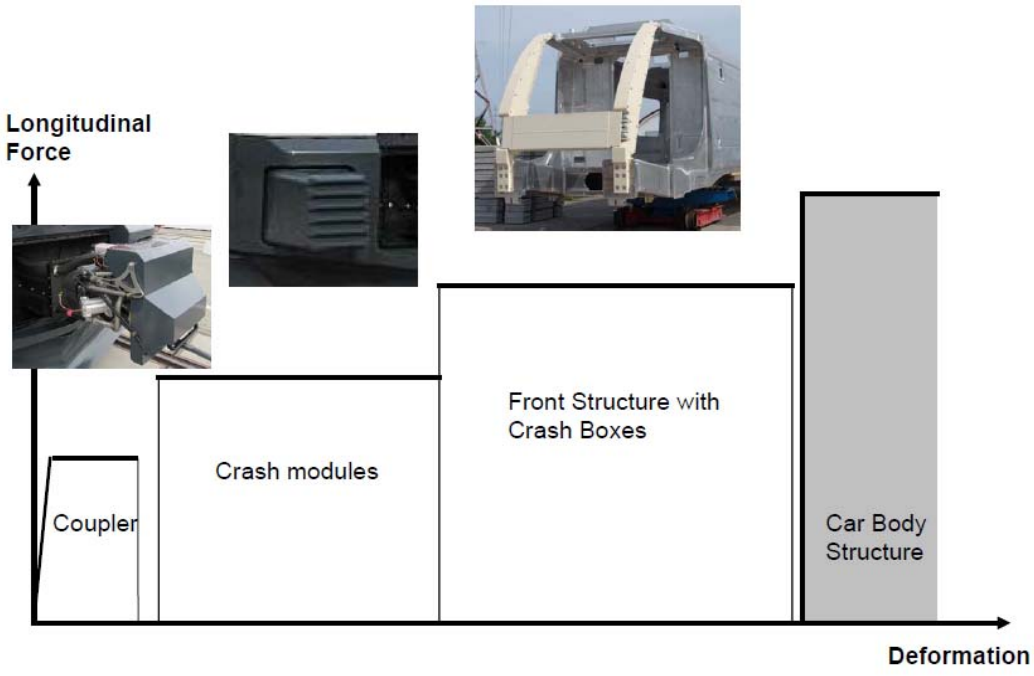

[43]

The force-displacement behavior of each element can be determined from design specifications, finite element model results, full-scale testing, or a combination of these. The design specification provides a range for the equipment behavior, but dynamic loading will affect the behavior of the system. Results from finite element analysis and full-scale testing [Figure 44] account for the dynamic effects, but require some smoothing.

Figure 44: Sample Comparison of Model and Test Results

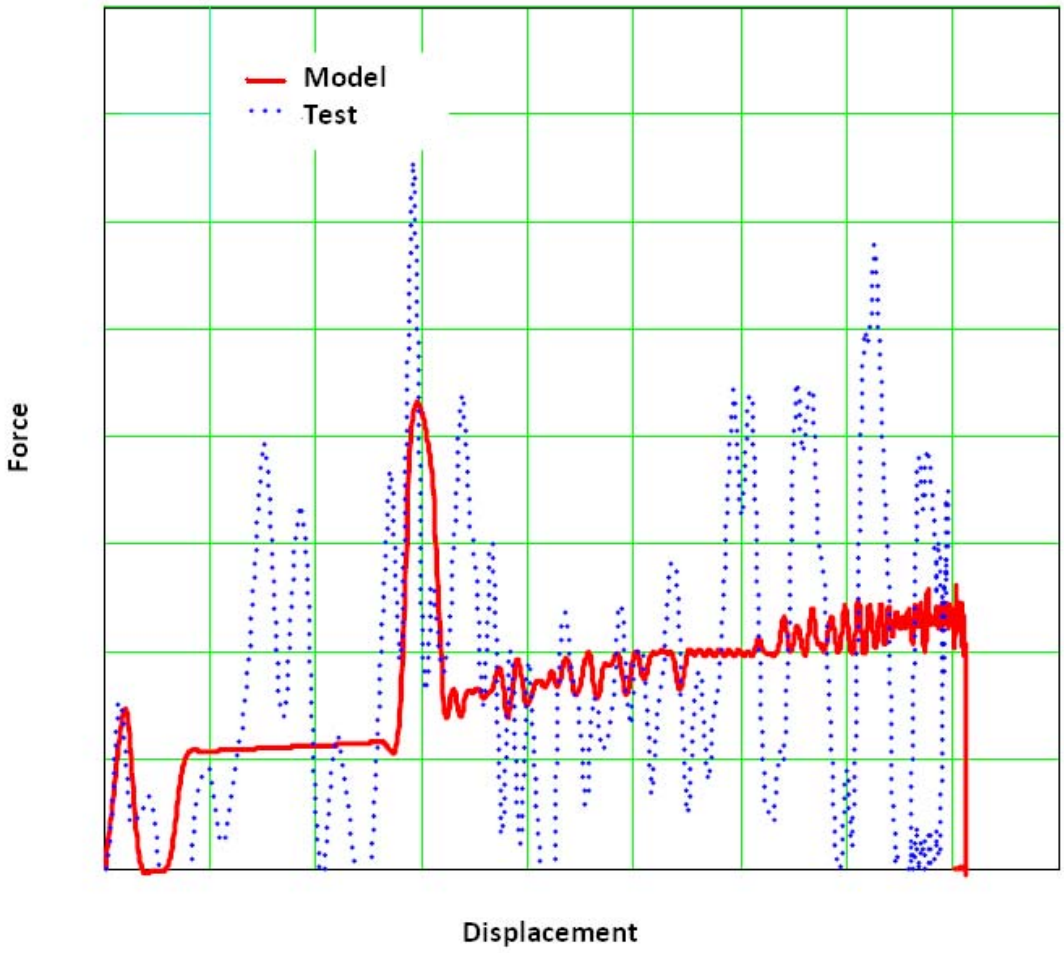

Specifications and results can be combined to approximate the crush behavior of the vehicle. The force-displacement characteristic in Figure 45 was assembled for the colliding end of the Acela powercar. The crush zone includes a draft gear, drawbar, and a front frame absorber. The unfiltered force-crush response of colliding end of the powercar was used to determine the general shape and stroke of the curve. Refinements were made using the values for the energy absorbed by each feature.

Figure 45: Colliding End Force Displacement of Acela Powercar

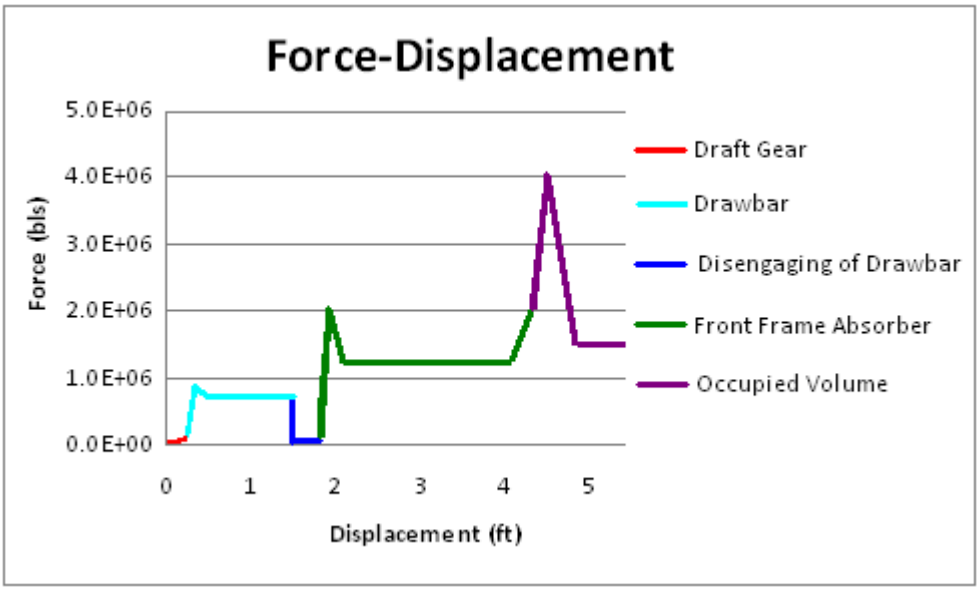

Many approaches have been taken for designing CEM equipment. No one approach is perfect, but each system provides some level of improvement to conventional structural crashworthiness. A CEM system can include a number of elements and features. Precise assembly of force crush curves for each high speed trainset is not feasible. A reasonable approximation can be made by including a number of common elements and applying some of the optimization principles that were developed in previous research [10, 13]. A baseline characteristic is constructed and alterations are made to account for variations in energy absorption capacity and crippling load.

Figure 46 shows the general outline of the force-displacement characteristic that is used for this thesis. A wide range of equipment is intended to be represented so the crush zone includes the basic features of the draft gear, pushback coupler, and primary energy absorber. No drop-out features are included for the sake of simplicity and ease of adjustment.

Figure 46: General Force-Displacement Characteristic

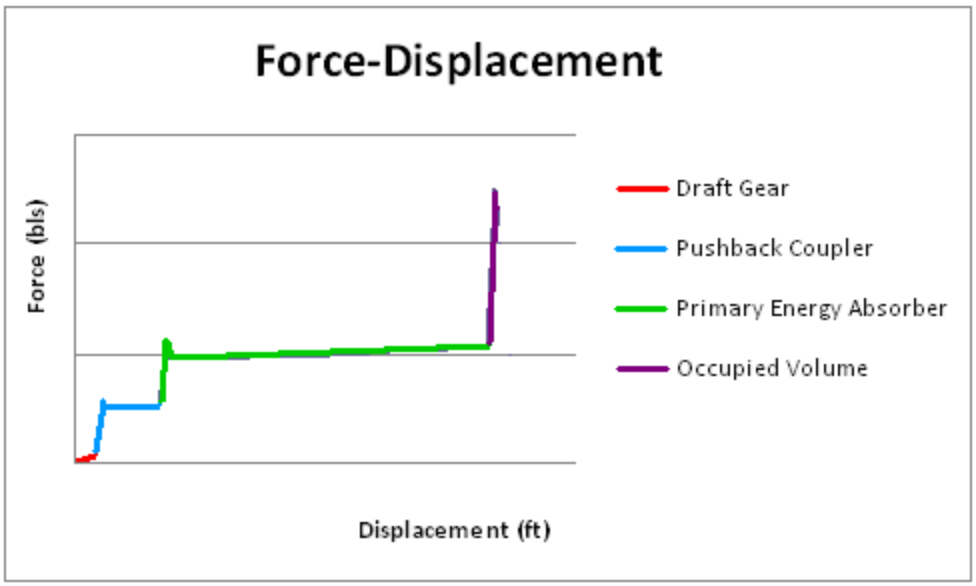

Appendix 4: Accident Survey

This accident survey compiles details of accidents involving high speed equipment. The accidents did not necessarily occur during high speed operation. Information is provided as available. Accidents are organized chronologically. The dates and locations are included to not only identify the incident, but to provide insight on the operating environment at the time. Conditions of the accident and the equipment involved describe how the equipment was threatened and what features were in place to mitigate the effects.

Accidents provide valuable information on the safety performance of equipment under real-world conditions. The severity and the conditions under which the collision occurred provide information on the forces that the equipment was subjected to in the collision. The extent of damage and the outcome of the collision for the passengers describe the crashworthiness of the system. Collisions play a large role in determining where improvements can be made to the system.

Multiple factors contribute to the severity of the collision. The speed of the incident, the colliding objects and any subsequent events will play a part in the outcome. The resulting damage to the equipment and the safety of the passengers will determine if crush was able to be controlled by the structure and passengers were able to safely ride out the collision. Accident details highlight

the strengths and weaknesses of the equipment to aid in design improvements for both the accident mitigation measures and accident prevention measures.

In order to determine an appropriate collision scenario, assumptions are made based on the category of accident. Train to train collisions, grade crossing collisions, and collisions with obstacles occur while the equipment is traveling on the track. For these cases collision forces can be assumed to be largely longitudinal in the direction of travel. In derailments, the equipment is no longer traveling on a designated path and loading conditions are unpredictable.

Location: Voiron, France [46]

Date: September 23, 1988

Equipment Involved: TGV-SE

Category: Grade Crossing

Closing Speed: 68 mph

Description: A heavy transport vehicle became stranded on the grade crossing and it struck by the passenger train. The power car and first trailing care were damaged, and the driving cab was crushed. There were 60 injuries and 1 fatality

Location: Mâcon-Loché, France [47]

Date: December 14, 1992

Equipment Involved: TGV-SE

Category: Derailment

Speed: 168 mph

Description: A flat spot on the wheel caused one truck to derail as it passed through the station. There were 27 slight injuries.

Location: Haute-Picardie, France [47].

Date: December 21, 1993

Equipment Involved: TGV-R

Category: Derailment

Speed: 182 mph

Description: Heavy rains created a sink hole leaving a section of track unsupported. As the train passed over the gap, the engineer felt the bump and applied the brakes, the last four passenger cars and the rear power car derailed. There was one slight injury [Figure 47].

Figure 47: Sink Hole Causing the Haute-Picardie Incident

Photo: Jean-Marie Hervio / Le Parisien Libéré

Location: Vitré, France [47]

Date: August 10, 1995

Equipment Involved: TGV-A

Category: Grade Crossing

Closing Speed: 87 mph

Description: Tractor-trailer with farm equipment became stranded at the crossing, and was struck by a passenger train. There were two slight injuries [Figure 48].

Figure 48: Colliding End of the Power Car at Vitré

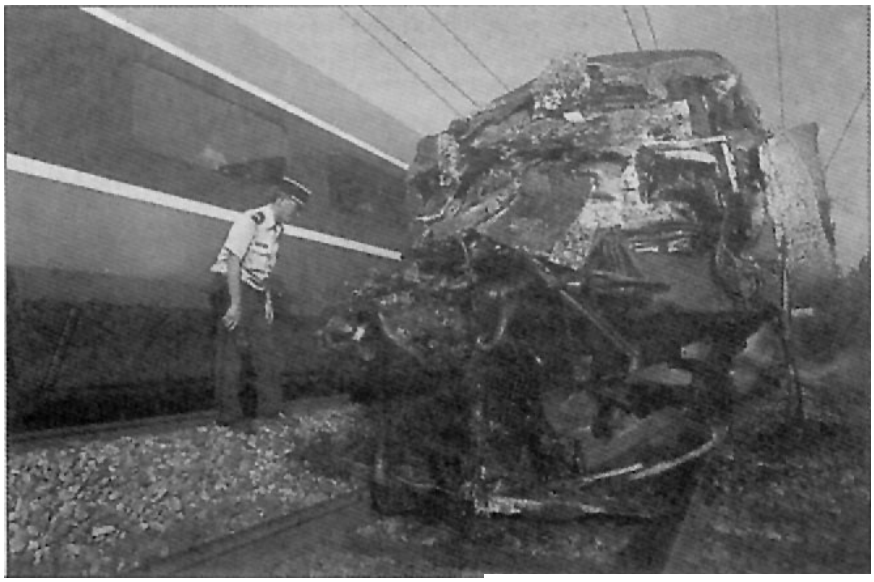

Photo: David Adémas (Ouest France)

Location: Bierne, France [47]

Date: September 25, 1997

Equipment Involved: TGV-R

Category: Grade Crossing

Closing Speed: 81 mph

Description: A paving machine becomes stuck on the grade crossing and is struck by the passenger train. The leading power car is destroyed and four passenger cars derail. There were seven slight injuries [Figure 49].

Figure 49: Colliding End of the Power Car at Bierne

Photo: Pascal Rossignol (Reuters)

Location: Neau, France [47]

Date: November 19, 1997

Equipment Involved: TGV-A

Category: Grade Crossing

Closing Speed: 87 mph

Description: A tractor-trailer becomes disabled on the grade crossing and is struck by the passenger train. One truck derails. There were 6 slight injuries [Figure 50].

Figure 50: Colliding End of the Power Car at Neau

Photo: Valéry Hache (AFP)

Location: Hoeven, Netherlands [47]

Date: May 9, 1998

Equipment Involved: Thalys PBKA

Category: Grade Crossing

Closing Speed: unknown

Description: A truck attempts to cross at an unprotected grade crossing and is struck by the passenger train. The power car and two passenger cars derail. There were six slight injuries [Figure 51].

Figure 51: Damage to the Equipment at Hoeven

Photo: Arie Kievit/Volkskrant

Location: Eschede, Germany [48]

Date: June 3, 1998

Equipment Involved: ICE 1

Category: Derailment

Speed: approximately 124 mph

Description: A piece of wheel peels away and causes damages to the floor of the car and the track. The train begins to derail as it passes under a bridge. The powercar and the second car clear the bridge, the third strikes the bridge and the fourth car separates and rolls away from the bridge. The bridge then collapses onto the fifth and sixth cars. The remaining cars strike the wreckage. There were 101 fatalities [Figure 52].

Figure 52: Wreckage at Ecshede

Location: Guipavas, France [47]

Date: November 28, 1998

Equipment Involved: TGV-A

Category: Grade Crossing

Closing Speed: 75 mph

Description: A truck becomes stranded at a grade crossing and is struck by a passenger train. The lead power car was damaged. There were no injuries [Figure 53].

Figure 53: Damage to the Power Car at Guipavas

Photo: Eugene Le Droff/Le Telegramme

Location: Ladbroke Grove, UK [49]

Date: January 5, 1999

Equipment Involved: BR Class 165 DMU and Class 43 HST

Category: Train to train

Closing Speed: 130 mph

Description: The DMU passes a red signal and strikes the HST. The first car of the HST is badly damaged and the first car of the DMU is destroyed. A fire results, causing more extensive damage to the HST. There were 227 serious injuries and 31 fatalities.

Location: Brühl, Germany [50]

Date: February 6, 2000

Equipment Involved: ICE equipment

Category: Derailment

Speed: 75 mph

Description: The passenger train speeds over a switch and derails. Derailed equipment leaves the right of way and is damaged by the platform and residential buildings. There were 149 injuries, some serious; and 9 fatalities.

Location: Laval, France [47]

Date: January 5, 2001

Equipment Involved: TGV-A

Category: Derailment

Speed: 74 mph

Description: A mudslide covers the tracks and the power car derails. There were no injuries.

Location: Torredembarra, Spain [51]

Date: March 30, 2002

Equipment Involved: Euromed

Category: Train to train

Closing Speed: 65 mph

Description: A high speed train and a regional passenger train collided. There were 142 injuries and 2 fatalities.

Location: Istein, Germany [52]

Date: April 1, 2004

Equipment Involved: ICE 3

Category: Collision with an obstacle

Closing Speed: unknown

Description: A tractor fell on the tracks and was struck by the passenger train. There were no injuries.

Location: Saint Romain en Gier, France [53]

Date: April 5, 2004

Equipment Involved: TGV-Duplex

Category: Train to Train

Closing Speed: 18 mph

Description: An overnight maintenance train has been delayed and routed onto the track of the morning passenger train. There is some damage to the power head. There were 2 slight injuries [Figure 54].

Figure 54: Damage to the Equipment at Saint Romain en Gier

Location: Thun, Switzerland [54]

Date: April 28, 2006

Equipment Involved: ICE 1

Category: Train to Train

Closing Speed: 35 mph

Description: Confusion is caused by construction at the station and a passenger train and freight train collide. Automatic breaking slows the collision. There were injuries to seven passengers and the drivers [Figure 55]

Figure 55: Damage to the Powercar at Thun

Location: München, Germany [55]

Date: July 24, 2007

Equipment Involved: ICE

Category: Collision with an obstacle

Closing Speed: 122 mph

Description: The inter city train strikes a section of rail that had fallen into the path of the train. The control car derails. There were 5 serious injuries.

Location: Tossiat, France [56]

Date: December 29, 2007

Equipment Involved: TGV-SE

Category: Grade Crossing

Closing Speed: 62 mph

Description: A heavy truck becomes stuck at a grade crossing and is struck by the passenger train. There were 22 slight injuries [Figure 56].

Figure 56: Damage to the Powercar at Tossiat

Location: Fulda, Germany [57]

Date: April 26, 2008

Equipment Involved: ICE 1

Category: Collision with an obstacle

Closing Speed: 130 mph

Description: The passenger train strikes a flock of sheep as it's leaving a tunnel. The control car derails. There were 21 serious injuries and 17 slight injuries [Figure 57].

Figure 57: Damage to the Powercar at Fulda

Location: Lambrecht, Germany

Date: August 17, 2010

Equipment Involved: ICE

Category: Collision with an obstacle

Closing Speed: unknown

Description: A garbage truck slides down and embankment and lands on the tracks and is struck by the passenger train. There was one serious injury [58].

The collision conditions and the injuries and fatalities associated with the collisions are summarized in Table 8. A majority of these collisions involve longitudinal loading conditions. In most of these cases, the speeds were low enough or the collision object was small enough that the equipment was capable of protecting the passengers in the collision. For the most severe collisions however accident mitigation measures cannot fully protect the passengers. These accidents must be prevented.

Table 8: Summary of Accident Survey

Location	Type of Collision	Speed of Collision (mph)	Injuries	Fatalities
Voiron	Grade Crossing	68	60	1
Mâcon-Loché	Derailment	168	27	0
Haute-Picardie	Derailment	182	1	0
Vitré	Grade Crossing	87	2	0
Bierne	Grade crossing	81	7	0
Neau	Grade Crossing	87	6	0
Hoeven	Grade Crossing	--	6	0
Eschede	Derailment	124		101
Guipavas	Grade Crossing	75	0	0
Ladbroke Grove	Train to train	130	227	31
Brühl	Derailment	75	149	9
Laval	Derailment	74	0	0
Torredembarra	Train to train	65	142	2
Istein	Collision with Obstacle	--	0	0
Saint Romain en Gier	Train to train	18	2	0
Thun	Train to train	35	9	0
München	Collision with obstacle	122	5	0
Tossiat	Grade Crossing	62	22	0
Fulda	Collision with obstacle	130	38	0
Lambrecht	Collision with obstacle	--	1	0

[1] Lewis, J.H., “Structural Crashworthiness Overview” Symposium on Rail Vehicle Crashworthiness, Cambridge, Massachusetts, USA, June 1996.

[2] Tyrell, D., Jacobsen, K., Martinez, E., “A Train-to-Train Impact Test of Crash Energy Management Passenger Rail Equipment: Structural Results,” American Society of Mechanical Engineers, Paper No. IMECE2006-13597, November 2006.

[3] Smith, R.A., “Crashworthiness oF Trains: Principles and Progress,” AMD-Vol. 210/BED – Vol. 30, Crashworthiness and Occupant Protection in Transportation Systems, ASME 1995.

[4] Scholes, A., “Vehicle Design Loads and Structural Crashworthiness,” IMechE Conference on Railway Vehicle Body Structures, Paper C248/85, 147-154, 1985.

[5] Scholes, A., Lewis, J.H., “Development of Crashworthiness for Railway Vehicle Structures,” Proc. Instn Mech. Engrs, Part F: J. Rail and Rapid Transit, 207(F1), 1-16, 1993.

[6] Lewis, J.H., Rasaiah, W.G., “Validation of Measures to Improve Rail Vehicle Crashworthiness,” Proc. Instn Mech. Engrs, Part F: J. Rail and Rapid Transit, 216(F1), 73-85, 1996.

[7] Tyrell, D.C., Severson, K.J., Marquis, B.P., “Train Crashworthiness Design for Occupant Survivablilty,” American Society of Mechanical Engineers, AMD-Vol. 210, BED-Vol. 30, pp. 59-74, 1995.

[8] Tyrell, D.C., Perlman, A.B., "Evaluation of Rail Passenger Equipment Crashworthiness Strategies," Transportation Research Record No. 1825, pp. 8-14, National Academy Press, 2003.

[9] Priante, M., Tyrell, D., Perlman, A.B., 'The Influence of Train Type, Car Weight, and Train Length on Passenger Train Crashworthiness," American Society of Mechanical Engineers, Paper No. IMECE2005-70042, March 2005

[10] Priante, M., “Influence of Train Parameters on Crashworthiness Performance of Passenger Trains,” Tufts University Undergraduate Honors Thesis, May 2004.

[11] Jacobsen, K., Severson, K., Perlman, A.B., "Effectiveness of Alternative Rail Passenger Equipment Crashworthiness Strategies," American Society of Mechanical Engineers, Paper No. JRC2006-94043, April 2006.

[12] Carolan, M., Perlman, A.B., Tyrell, D., "Performance Efficiency of a Crash Energy Management System," Proceedings of the 2007 ASME/IEEE Joint Rail Conference & Internal Combustion Engine Spring Technical Conference, JRCICE2007-40064, March 2007.

[13] Carolan, M., “Performance Efficiency of Crash Energy Management Systems,” Tufts University Undergraduate Honors Thesis, May 2006.

[14] Mallon, P., Perlman, B.A., Tyrell, D., "The Influence of Manufacturing Variations on a Crash Energy Management System" American Society of Mechanical Engineers, Paper No. RTDF2008-74021, September 2008

[15] Scholes, A., Lewis, J.H., “Development of Crashworthiness for Railway Vehicle Structures,” Proc. Instn Mech. Engrs, Part F: J. Rail and Rapid Transit, 216(F1), 1-16, 1993.

[16] Lu, G. “Energy Absorption Requirement for Crashworthy Vehicles” Proc. Instn Mech. Engrs, Part F: J. Rail and Rapid Transit, 216(F1), 31-39, 2002.

[17] EN 15227 Railway Applications—Crashworthiness Requirements for Railway Vehicle Bodies, Ref. No. prEN 15227:2007:E.

[18] Cleon, L. M., Legait, J., Villemin, M. "SNCF Structural Crashworthiness Design Strategy" Symposium on Rail Vehicle Crashworthiness, Cambridge, Massachusetts, USA, June 1996.

[19] US Department of Transportation, Federal Railroad Administration, "49 CFR part 238 Subpart E – Specific Requirements for Tier II Passenger Equipment," Federal Register, September 9, 1999.

[20] US Department of Transportation, Federal Railroad Administration, "Technical Criteria and Procedures for Evaluating the Crashworthiness and Occupant Protection Performance of Alternatively-Designed Passenger Rail Equipment for Use in Tier I Service," DOT/FRA/ORD-xx/xx.

[21] Sutton, A., "The Development of Rail Vehicle Crashworthiness" Proc. Instn Mech. Engrs, Part F: J. Rail and Rapid Transit, 216(F2), 97–108, 2001.

[22] Lu, G., "Collision Behaviour of Crashworthy Vehicles in Rakes," Proc. Instn Mech. Engrs, Part F: J. Rail and Rapid Transit, 213 (F1), 143-160,1999.

[23] Carolan, M., Perlman, A.B., Tyrell, D., "Performance Efficiency of a Crash Energy Management System," Proceedings of the 2007 ASME/IEEE Joint Rail Conference & Internal Combustion Engine Spring Technical Conference, JRCICE2007-40064, March 2007.

[24] Severson, K., "Development of Models to Estimate Rail Vehicle Impact Tests," Tufts University Masters Thesis, November 2000.

[25] Technical Specification for Interoperability TSI HS RS, version 2008.

[26] Alstom Transport Presentation INNOTRANS – Berlin September 2008

[27] Alstom Transport Presentation FRA Engineering Task Force Meeting – Cambridge, Massachusetts, USA, October 2010.

[28] "Automotrice à grande vitesse." *Wikipedia, The Free Encyclopedia*. Wikimedia Foundation, Inc. 18 August 2011. Web. Accessed on 27 September 2011. <http://en.wikipedia.org/wiki/Automotrice_%C3%A0_grande_vitesse>

[29] "AVE S-102 – Spain" Project Overview and Technical Data. *Bombardier Transportation*. Bombardier Inc, n.d. Web. Accessed on 27 September 2011. <http://bombardier.com/en/transportation/products-services/rail-vehicles/high-speed-trains/ave-s-102---spain?docID=0901260d8001067e#>

[30] "AVE Class 102," *Wikipedia, The Free Encyclopedia*. Wikimedia Foundation, Inc. 9 August 2011. Web. Accessed on 27 September 2011. <http://en.wikipedia.org/wiki/AVE_Class_102>

[31] "High Speed Trainset ICE 2, Germany." References. *Siemens Mobility.* Siemens AG. 2002 Web. Accessed on 27 September 2011.

<http://www.mobility.siemens.com/apps/references/index.cfm?z=1&do=app.detail&referenceID=383&IID=1>

[32]"ICE 3" *Wikipedia, The Free Encyclopedia*. Wikimedia Foundation, Inc. 24 September 2011. Web. Accessed on 27 September 2011. <http://en.wikipedia.org/wiki/ICE_3>

[33] "High Speed - Talgo 250 trainset with Series VII cars" Talgo 250 Brochure. *Talgo America*. Talgo, 2010. Web. Accessed on September 27, 2011.< http://talgoamerica.com/High-Speed.aspx>

[34] "TGV Réseau." Trainweb,org. TGVweb. n.d. Web. Accessed on 27 September 2011. <http://www.trainweb.org/tgvpages/tgvreseau.html>

[35] "TGV Duplex" Trainweb.org. TGVweb. 29 March 1998. Web. Accessed on 27 September 2011. < http://www.trainweb.org/tgvpages/duplex.html>

[36] Nippon Sharyo Presentation FRA Engineering Task Force Meeting – Cambridge, Massachusetts, USA, October 2010.

[37] "V250 High Speed Railways Prodotti " V250 Brochure. *Ansaldo Breda*. Ansaldo Breda, a Finmeccanica Company, n.d. Web. Accessed on 27 September 2011. <http://www.ansaldobreda.it/upload/allegati_prodotti/51_ITA_v250.pdf>

[38] "High Speed Trainset Velaro CRH3" References. *Siemens Mobility.* Siemens AG. n.d. Web. Accessed on 27 September 2011. <http://www.mobility.siemens.com/apps/references/index.cfm?z=1&do=app.detail&referenceID=1446&IID=1>

[39] "High Speed Trainset Velaro RUS Sapsan, Russia." References. *Siemens Mobility.* Siemens AG. n.d. Web. Accessed on 27 September 2011. <http://www.mobility.siemens.com/apps/references/index.cfm?z=1&do=app.detail&referenceID=1447&IID=1>

[40] Siemens AG Presentation FRA Engineering Task Force Meeting – Cambridge, Massachusetts, USA, October 2010.

[41] Bombardier Presentation FRA Engineering Task Force Meeting – Cambridge, Massachusetts, USA, October 2010.

[42] "British Rail Class 180" *Wikipedia, The Free Encyclopedia*. Wikimedia Foundation, Inc. 21 September 2011. Web. Accessed on 27 September 2011. <http://en.wikipedia.org/wiki/British_Rail_Class_180>

[43] Stadler Presentation, FRA Engineering Task Force Meeting, Cambridge, Massachusetts, USA, October 2010.

[44] Contract No. EP142-06 Metrolink Commuter Rail Cars – Technical Specification, Issued 03/14/06.

[45] Ansaldo Breda Presentation FRA Engineering Task Force Meeting – Cambridge, Massachusetts, USA, October 2010.

[46] Cleon, L. M., Legait, J., Villemin, M. "SNCF Structural Crashworthiness Design Strategy" Symposium on Rail Vehicle Crashworthiness, Cambridge, Massachusetts, USA, June 1996.

[47] "TGV Accidents." *Trainweb.org*. TGVweb. June 2000. Web. Accessed on 27 September 2011. <http://www.trainweb.org/tgvpages/wrecks.html>

[48] "Eschede Train Disaster," *Wikipedia, The Free Encyclopedia*. Wikimedia Foundation, Inc. 26 September 2011. Web. Accessed on 27 September 2011. <http://en.wikipedia.org/wiki/Eschede_train_disaster>

[49] The Train Collision at Ladbroke Grove 5 October 1999, A report of the HSE investigation, Health and Safety Executive, 2000.

[50] Untersuchungsbericht Entgleisung des D 203 im Bahnhof Brühl am 06.02.2000, Eisenbahn-Bundesamt Der Beauftragte für Unfalluntersuchung, April 2000.

[51] "Holiday Trains Crash in Spain." *bbc.co.uk*. BBC News Europe. 1 April 2002. Web. Accessed on September 27, 2010. <http://news.bbc.co.uk/2/hi/europe/1902977.stm>

[52] "Intercity-Express," *Wikipedia, The Free Encyclopedia*. Wikimedia Foundation, Inc. 24 September 2011. Web. Accessed on 27 September 2011. <http://en.wikipedia.org/wiki/Intercity-Express#Other_accidents>

[53] Rapport d'enquête technique sur l'accident ferroviaire du 5 avril 2004 à Saint-Romain-en-Gier, Bureau d'Enquêtes sur les Accidents de Transport Terrestre, Rapport n°BEATT-2004-002, 2004.

[54] "Kollision zwischen dem ICE Nr. 278 und einer unbegleiteten Rangierfahrt mit 2 Re 465 in Vst. von Freitag, 28. April 2006 in 3600 Thun BE," Schlussbericht der Unfalluntersuchungsstelle Bahnen und Schiffe, Reg. Nr. 06042801, 2007.

[55] Eisenbahn-Unfalluntersuchungsstelle beim Bundesministerium für Verkehr, Bau und Stadtentwicklung, "Strecke: München - Augsburg zwischen München Lochhausen und Gröbenzell," European Rail Agency Database of Interoperability and Safety, Investigation Notification Form, Report ID: DE-391

[56] Rapport d'enquête technique sur la collision entre un TGV et un convoi exceptionnel survenue le 19 décembre 2007 au passage à niveau 34 à Tossiat (01), Bureau d'enquêtes sur les Accidents de transport terrestre, avril 2009.

[57] Untersuchungsbericht Zugkollision mit anschl. Entgleisung des ICE 885 im Landrückentunnel am 26.04.2008, Bundesministerium für Verkehr, Bau und Stadtentwicklung, Eisenbahn-Unfalluntersuchungsstelle des Bundes, 2010.

[58] Eisenbahn-Unfalluntersuchungsstelle beim Bundesministerium für Verkehr, Bau und Stadtentwicklung, "Lambrecht (Pfalz)- Neustadt (Weinstraße); Strecke 3280; in km 71,6," European Rail Agency Database of Interoperability and Safety, Investigation Notification Form, Report ID: DE-971